JACS
JOURNAL OF THE AMERICAN CHEMICAL SOCIETY
pubs.acs.org/JACS
Article

Kinetic DNA Self-Assembly: Simultaneously Co-folding Complementary DNA Strands into Identical Nanostructures

Mengxi Zheng, Zhe Li, Longfei Liu, Mo Li, Victoria E. Paluzzi, Jong Hyun Choi, and Chengde Mao*

Cite This: https://doi.org/10.1021/jacs.1c09925
Read Online

ABSTRACT: DNA origami is a powerful method for constructing DNA nanostructures. It requires long single-stranded DNAs. The preparation of such long DNA strands is often quite tedious and has a limited production yield. In contrast, duplex DNAs can be easily prepared via enzymatic reactions in large quantities. Thus, we ask a question: can we design DNA nanostructures in such a way that the two complementary strands can simultaneously fold into the designed structures in the same solution instead of hybridizing with each other to form a DNA duplex? By engineering DNA interaction kinetics, herein we are able to provide multiple examples to concretely demonstrate a positive answer to this question. The resulting DNA nanostructures have been thoroughly characterized by electrophoresis and atomic force microscopy imaging. The reported strategy is compatible with the DNA cloning method and thus would provide a convenient method for the large-scale production of the designed DNA nanostructures.

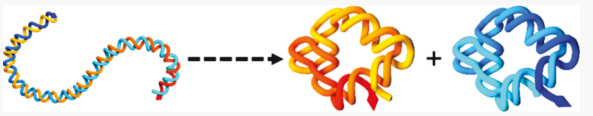

INTRODUCTION

DNA nanostructures are highly programmable and nanoscale-controllable and find a wide variety of applications in biology, medicine, materials science, and computing.[1,2] Recently, collective efforts have been devoted to developing strategies to assemble single-component DNA nanostructures by folding long single-stranded DNAs (ssDNAs). Up to 10 000-nucleotide (nt)-long ssDNA has been demonstrated to fold into a defined nanostructure,[3−5] suggesting that this approach could reach high complexities. Compared with multistrand DNA nanostructures, single-component DNA nanostructures have great advantages in terms of preparation, including (i) the elimination of stoichiometry issues, (ii) compatibility with molecular cloning, and (iii) no concentration limits. However, one major challenge is how to prepare long ssDNAs. Such a long DNA strand is generated by DNA polymerases in the form of duplexes, followed by specifically keeping one strand while removing the complementary strand, for example, asymmetric PCR,[6,7] asymmetric exonuclease digestion,[8] affinity separation,[9] and selective precipitation.[10] Alternatively, ssDNAs can also be biotechnologically generated via cloning into bacteriophages with ssDNA genomes.[11−13] All existing methods are tedious and have a limited production amount. In most cases, only one strand of a duplex can be used, so 50% of the DNAs are wasted. Though RNA seems to be a potential solution,[5,14−16] the poor chemical and biological stability casts concern over its potential. To solve this problem, we ask a simple question: can we devise a strategy that will allow the two complementary strands of a double-stranded DNA (dsDNA) duplex to simultaneously fold into the same nanostructures (at the nanoscale) in one pot? Herein, we provide a positive answer to this question.

RESULTS AND DISCUSSION

Here, we describe a strategy to prepare two single-component DNA nanostructures that are different in sequence but identical in morphology and shape by one pot, cofolding the two complementary ssDNAs of a DNA duplex (Figure 1). The experimental process is very simple and can be completed within a few minutes. A DNA duplex is thermally denatured into two strands, which, upon a thermal quench, quickly but separately self-fold into hairpin-rich, intermediate, secondary structures and then further form desired nanostructures via internal bubble−bubble interactions. The two nanostructures folded from the two complementary strands are identical to each other on the nanometer scale. We have demonstrated that 200- to 1800-nt-long DNA can successfully fold into the designed nanostructures.

The key to this strategy is to design the self-folding path to be both kinetically favorable and thermodynamically metastable. Each involved DNA strand has a very strong secondary structure, in which most of the bases exist in base pairs, and only a very small number of bases are left in single-stranded loops. Since folding into such a secondary structure is an intramolecular process, it is expected to be very fast. In contrast, the hybridization of two complementary strands into a duplex is an intermolecular process, which is expected to be much slower at the experimental DNA concentration (∼1

Received: September 18, 2021

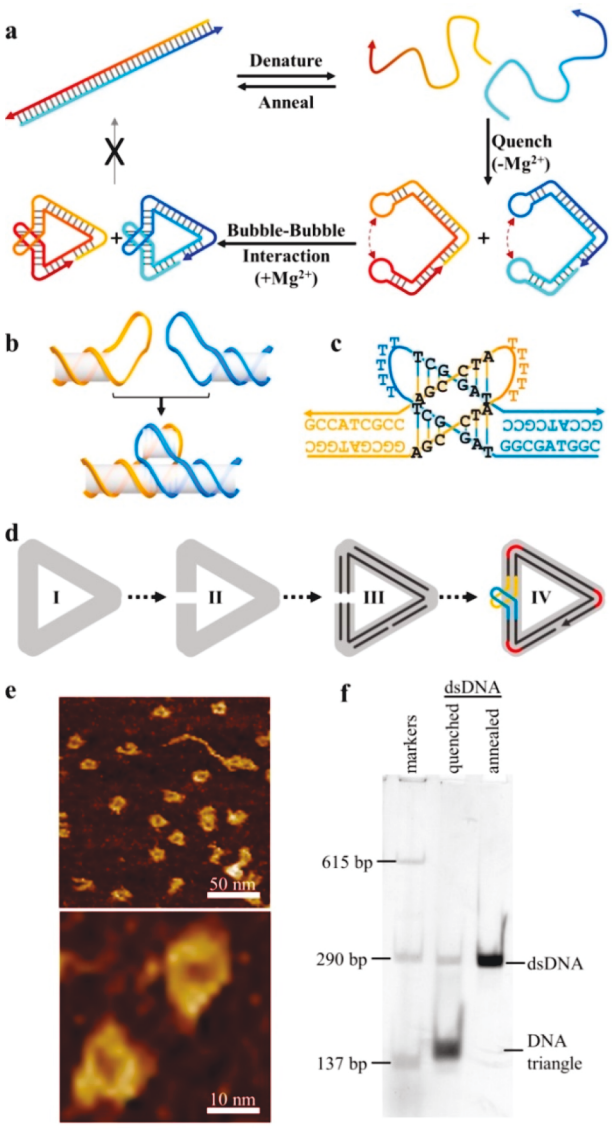

Figure 1. One-pot cofolding of a pair of complementary DNA strands into identical nanostructures as exemplified by a pair of triangles. (a) Path from a DNA duplex to a pair of identical single-component DNA nanostructures. (b) General scheme and (c) a specific example of internal bubble−bubble interactions. (d) Retro-design route of a single-component DNA triangle. (e) Atomic force microscopy (AFM) images of DNA triangles at two different magnifications. (f) Native polyacrylamide gel electrophoresis (PAGE) analysis of the formation of DNA triangles in the presence of Mg^{2+} and PCR primers.

μM). Thus, cofolding into the designed nanostructures is kinetically favorable. Furthermore, in the final structures, only a very small number of bases remain as unpaired bases in 5-nt-long loops (either T5 or A5). Though T5 and A5 loops are complementary to each other, it is unlikely for them to hybridize with each other because of the topological/geometrical restraints. Thus, the final resulting pair of nanostructures is stable, and they will not hybridize with each other to form duplexes.

The bubble−bubble interaction is an essential element of this strategy. It allows two parts of the same DNA strand to intramolecularly interact with each other over a long distance, and it does not rely on DNA free ends. A bubble−bubble interaction is formed by two hairpins (Figure 1b,c).[17,18] Each hairpin contains a 17-nt loop in which a T5 (or A5) region flanks two 6-base pair (bp) interacting regions on each side. The 6-bp regions are designed to be complementary to the 6-bp region of its pairing bubble. Two bubbles can recognize and base-pair with each other by the hybridization of the two 17-nt loops, and both T5 regions remain unpaired. Since each pair of interacting bubble pairs involves a relatively large number of base pairs (12 bps, to be specific), it is quite easy to design specific interacting sequences. In this work, 13 orthogonally interacting bubble pairs have been designed (Table S1). The interactions among 13 pairs of bubbles are confirmed by native polyacrylamide gel electrophoresis, PAGE (Figure S1). The heterodimer bands were observed for each pair of bubbles, indicating that the interactions successfully formed.

For a given nanostructure, we have developed a retro-design process to design the corresponding DNA molecule that will produce these desired nanostructures (Figure 1d). It is exemplified as designing DNA triangles and involves four stages. A triangle shape (I) is the target structure. It can be viewed as three rods linked into a closed structure and is not compatible with products from PCR or restriction digestion. They have free ends, so a nick is introduced into the structure (II). Each rod is replaced with a DNA duplex (III). Then ssDNA loops are added to link DNA segments into one long strand (IV). The final structure contains one and only one long DNA strand, which goes through every rod twice (forming duplexes). The resulting long DNA can be prepared by PCR amplification or cloned into a plasmid for amplification by bacteria. Note that the sharp, localized turns at the vertexes are realized by ssDNA loops, which can introduce sharp K-turns into DNA duplexes. The loop lengths depend on the desired angles and shapes. The nick positions are connected by bubble−bubble interactions.

We first tested this approach by designing a 264-nt DNA triangle (Figures 1, S2, and S3). The corresponding dsDNA with designed sequences was heated to 95 °C for 5 min to be denatured into two separate ssDNAs and quickly quenched in an ice bath for 5 min. Mg^{2+} (10 mM) was then added to support bubble−bubble interactions (Figure 1a). The triangular structures contain two PCR primer binding regions, 28-nt and 23-nt long, at the 5′- and 3′- ends, respectively, outside the triangular structures (Figure S2). Without any protection, the dangling ends will serve as toeholds to bring the two complementary triangles together and hybridize into a duplex. To prevent such undesired hybridization, we include excess amounts of the PCR primers in the solution. The primers will bind to the dangling tails and stabilize the triangular structures (Figure S4). The formation of the DNA triangles was confirmed by atomic force microscope (AFM) visualization (Figure 1e). The triangularly shaped particles, with a size of about 11 nm (consistent with the designed triangles), were randomly distributed on the surface. Using native PAGE in the presence of 10 mM Mg^{2+}, the heat-quenched products migrated much faster than the annealed dsDNA, which indicated that the heat-quenched products were the compact, one-strand-containing DNA triangles (Figure 1f). Estimated from the band intensities by ImageJ software, the folding efficiency of DNA triangles is 87.6%. In the absence of Mg^{2+}, the heat-quenched product also migrated faster than the dsDNA, suggesting that the products were one-stranded (Figure S3). However, they migrated much more slowly than the folded DNA triangles, indicating that products without Mg^{2+} were loosely packed intermediates as shown in Figure 1a

https://doi.org/10.1021/jacs.1c09925
J. Am. Chem. Soc. XXXX, XXX, XXX−XXX

and lacked bubble−bubble interactions, which was Mg^{2+}-dependent. Interestingly, dsDNA from the PCR amplification mixture, without any purification, could be directly used to prepare DNA triangles (Figure S3). We also found that low DNA concentration (Figures S5 and S6) and fast quenching (Figure S7) would suppress dsDNA formation. After being incubated at high temperature for a protracted amount of time, the triangles will gradually be converted to DNA duplexes (Figures S8−S10).

We further applied this strategy for moderately complex DNA nanostructures—2-square, 4-square, and 10-square—which, as the names imply, contain 2 (393 nts), 4 (647 nts), and 10 (1809 nts) squares, respectively (Figure 2). In these

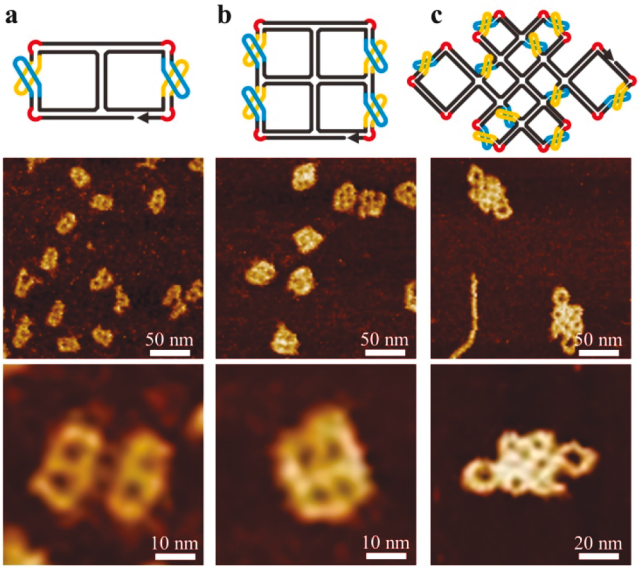

Figure 2. Complex DNA nanostructures. (a) 2-squares, (b) 4-squares, and (c) 10-squares. For each structure, the structural scheme is shown at the top and a pair of AFM images at different magnifications are shown below.

nanostructures, more structural motifs are needed. In DNA 2-square, two pairs of bubbles, two three-way junctions, and four 90° turns are included (Figure S11). In the more complicated 4-square structure, four pairs of bubbles, four three-way junctions, one four-way junction, and four 90° turns are used (Figure S13) In the even more complicated 10-square, ten pairs of bubbles, nine four-way junctions, and fourteen 90° angles are involved (Figure S15).

We prepared the dsDNA 2-square with designed sequences by PCR and denaturing PAGE purification. Following the heat-quench protocol, the designed structure was readily formed in a high yield of 95.6% (Figures 2a and S12). Under AFM imaging, well-defined 2-square shapes with expected sizes (~7 nm wide and ~15 nm long) were observed. Native PAGE not only allowed for a quantitative estimation of the folding yields but also distinguished the well-folded, final, compact nanostructures in the presence of Mg^{2+} and the loosely packed intermediates in the absence of Mg^{2+} due to the Mg^{2+} dependence of the bubble−bubble interactions. Similarly, the unpurified PCR reaction mixtures also produced well-shaped designed nanostructures. Following the same protocol, well-shaped 4-square and 10-square particles were also directly observed in the unpurified PCR mixtures (Figure S18).

While being convenient for preparing dsDNAs, PCR is expensive. It would be cost-effective to prepare long dsDNAs by inserting them into replication vectors to be amplified in bacteria. It has already been demonstrated that the biotechnological preparation of single-stranded DNAs for nanoassembly is feasible as bacteriophages functioning as a cloning vehicle. Instead of using bacteriophages as cloning vectors for discontinuous amplification, we used plasmids as cloning vectors to prepare 4-square and 10-square nanostructures in a continuous manner. Briefly, the dsDNAs that coded 4-square and 10-square were separately cloned into a pUC19 plasmid. After amplification in *E. coli*, the recombinant plasmids were extracted and digested with restriction enzymes to release the desired dsDNA inserts, which were then purified by gel electrophoresis. Following the heat-quench process, the dsDNAs successfully folded into 4-square and 10-square nanostructures with folding yields of 93.3 and 100%, respectively (Figures 2b,c, S14, and S17). Note that the dsDNAs produced by plasmid amplification did not contain 28-nt and 23-nt primer binding regions at the 5′- and 3′-ends. Thus, primers were not introduced into the heat-quench samples.

The key feature of the current method is the capability to simultaneously fold two complementary ssDNAs into identical nanostructures in the same solution. To further prove this concept, asymmetric PCR (aPCR) reactions (one primer is present in a 10-fold greater quantity than the other) of the 4-square-coding dsDNA were performed to generate the two complementary ssDNAs separately (Figure S19), as evidenced by a native PAGE (Figure S20). Under AFM imaging, 4-square structures were observed in both samples. Thus, we confirmed that either of the two complementary ssDNAs can fold into the designed structure.

The success of this folding process not only relied on the design of the sequence/secondary structures but also critically depended on the experimental protocols, particularly the Mg^{2+} concentration during the quenching step. In the absence of Mg^{2+}, the correct folding yield reached nearly 100%; in contrast, in the presence of 10 mM Mg^{2+}, the folding yield dramatically decreased to ~17% (Figure 3). In a pair of parallel experiments with the 4-square structure, one route was to add Mg^{2+} to the DNA solution after the quenching step, and the other was to add Mg^{2+} to the DNA solution before the quenching step. In the end, the two samples had the same buffer composition, containing 10 mM Mg^{2+} (Figure 3a). Both AFM imaging and native PAGE analysis revealed that the results were dramatically different. Adding Mg^{2+} after quenching resulted in nearly exclusive 4-square structures. Quenching with Mg^{2+} produced a mixture of one-stranded 4-square structures and two-stranded DNA duplexes. We speculate that the observed difference is due to the stabilization effect of Mg^{2+} on duplexes. During the quenching process, the self-folding of ssDNA and the binding of two complementary ssDNAs were considered to be competing reactions. Mg^{2+} stabilizes DNA double helices and promotes the formation of dsDNAs, which leads to low self-folding efficiency. However, as long as the desired secondary structures correctly fold, the long hairpin structures topologically protect the ssDNA regions and the Mg^{2+} would promote bubble−bubble interactions, leading to the final structures.

https://doi.org/10.1021/jacs.1c09925
J. Am. Chem. Soc. XXXX, XXX, XXX−XXX

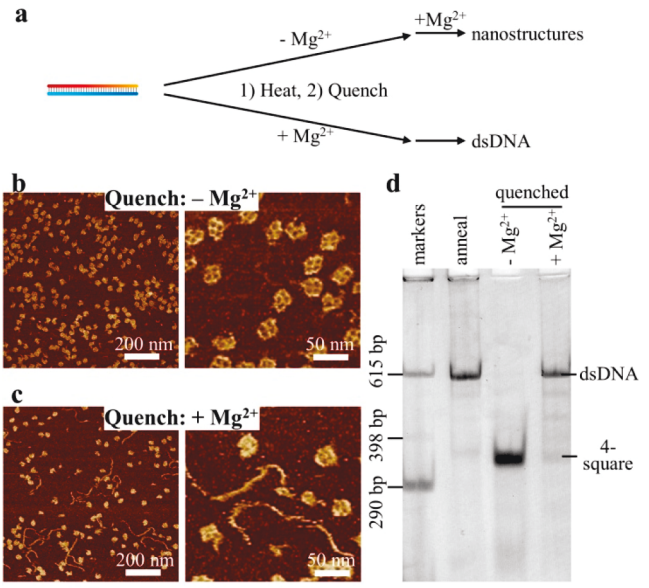

Figure 3. Effect of Mg^{2+} on the folding process. (a) Two different routes for the heat-quench process. AFM images of the samples quenched (b) in the absence and (c) in the presence of Mg^{2+}. (d) 4% native PAGE analysis of the effect of Mg^{2+} on the folding process.

CONCLUSIONS

To a certain extent, this strategy is developed from our previous approach where long ssRNAs can fold into designed nanostructures in a kinetically favorable way. RNAs first quickly folded into secondary structures rich in hairpins, which are thermodynamically stable and kinetically favorable. They further folded into desired tertiary nanostructures via internal, long-distance interactions (e.g., kissing loop interactions (KLs) or pRNA-like branching kissing loop interactions (bKLs)). From the previous RNA work to the current DNA work, there are two main challenges. (i) RNA strands are single-stranded, and complementary strands do not exist in the solution. The final RNA structures, as long as they form, are stable. Under the experimental conditions, the stable RNA duplex is not a competing alternative. However, in the current study, ssDNAs exist in complementary pairs. Thermodynamically, two-stranded DNA duplexes would be the most stable structures. The nanostructures can form only if the folding process is kinetically favored. The structures also need to be metastable and have high energy barriers to unfold. Similar situations are two complementary hairpin structures in a hybridization chain reaction (HCR) without initiator strands or in the strand displacement reactions without toeholds. The reactions could happen in principle according to thermodynamics but are nearly impossible in a reasonable experimental time period under our experimental conditions. (ii) RNAs have many well-established internal interactions (not requiring free ends), but DNAs do not. Fortunately, DNA bubble–bubble interactions resemble RNA KL interactions, even though they are much less commonly used.

We have demonstrated a convenient heat-quench method to prepare single-component DNA nanostructures from DNA duplexes within 15 min. The structure size ranges from 200 to 2000 nts. The main advantage of this method is that it avoids the tedious low-yield preparation of long ssDNAs. In addition, this method exploits both strands of a duplex, thus no DNA is wasted. However, it remains to be determined what complexity of the DNA nanostructures can be achieved by this approach, but it is very unlikely to rival conventional DNA origami. We envision that it is quite straightforward to adapt this method for the large-quantity production of DNA nanostructures via cloning DNA into bacteria.

ASSOCIATED CONTENT

Supporting Information

The Supporting Information is available free of charge at https://pubs.acs.org/doi/10.1021/jacs.1c09925.

Materials and methods and additional experimental data (PDF)

AUTHOR INFORMATION

Corresponding Author

Chengde Mao − *Department of Chemistry, Purdue University, West Lafayette, Indiana 47907, United States;* orcid.org/0000-0001-7516-8666; Email: mao@purdue.edu

Authors

Mengxi Zheng − *Department of Chemistry, Purdue University, West Lafayette, Indiana 47907, United States*

Zhe Li − *Department of Chemistry, Purdue University, West Lafayette, Indiana 47907, United States;* orcid.org/0000-0001-9402-4940

Longfei Liu − *Department of Chemistry, Purdue University, West Lafayette, Indiana 47907, United States;* orcid.org/0000-0002-5760-2964

Mo Li − *Department of Chemistry, Purdue University, West Lafayette, Indiana 47907, United States*

Victoria E. Paluzzi − *Department of Chemistry, Purdue University, West Lafayette, Indiana 47907, United States*

Jong Hyun Choi − *School of Mechanical Engineering, Purdue University, West Lafayette, Indiana 47907, United States*

Complete contact information is available at: https://pubs.acs.org/10.1021/jacs.1c09925

Notes

The authors declare no competing financial interest.

ACKNOWLEDGMENTS

This article is dedicated in memory of Prof. Nadrian (Ned) Seeman, the founder of Structural DNA Nanotechnology, for his inspiration, mentorship and friendship. This work was supported by the NSF (2025187 and 2107393).

REFERENCES

(1) Pinheiro, A. V.; Han, D.; Shih, W. M.; Yan, H. Challenges and opportunities for structural DNA nanotechnology. *Nat. Nanotechnol.* **2011**, *6*, 763−772.

(2) Seeman, N. C.; Sleiman, H. F. DNA nanotechnology. *Nat. Rev. Mater.* **2018**, *3*, 17068.

(3) Shih, W. M.; Quispe, J. D.; Joyce, G. F. A 1.7-kilobase single-stranded DNA that folds into a nanoscale octahedron. *Nature* **2004**, *427*, 618−621.

(4) Lin, C.; Wang, X.; Liu, Y.; Seeman, N. C.; Yan, H. Rolling circle enzymatic replication of a complex multi-crossover DNA nanostructure. *J. Am. Chem. Soc.* **2007**, *129*, 14475−14481.

(5) Han, D.; Qi, X.; Myhrvold, C.; Wang, B.; Dai, M.; Jiang, S.; Bates, M.; Liu, Y.; An, B.; Zhang, F.; Yan, H. Single-stranded DNA and RNA origami. *Science* **2017**, *358*, 6369.

(6) Gyllensten, U. B.; Erlich, H. A. Generation of single-stranded DNA by the polymerase chain reaction and its application to direct

sequencing of the HLA-DQA locus. *Proc. Natl. Acad. Sci. U. S. A.* **1988**, *85*, 7652−7656.
(7) Ellington, A. D.; Szostak, J. W. Selection in vitro of single-stranded DNA molecules that fold into specific ligand-binding structures. *Nature* **1992**, *355*, 850−852.
(8) Kujau, M. J.; Wölfl, S. Efficient preparation of single-stranded DNA for in vitro selection. *Mol. Biotechnol.* **1997**, *7*, 333−335.
(9) Hultman, T.; Stahl, S.; Homes, E.; Uhlen, M. Direct solid phase sequencing of genomic and plasmid DNA using magnetic beads as solid support. *Nucleic Acids Res.* **1989**, *17*, 4937−4946.
(10) Bowman, B. H.; Palumbi, S. R. [29] Rapid production of single-stranded sequencing template from amplified DNA using magnetic beads. *Methods Enzymol.* **1993**, *224*, 399−406.
(11) Praetorius, F.; Kick, B.; Behler, K. L.; Honemann, M. N.; Weuster-Botz, D.; Dietz, H. Biotechnological mass production of DNA origami. *Nature* **2017**, *552*, 84−87.
(12) Jia, Y.; Chen, L.; Liu, J.; Li, W.; Gu, H. DNA-catalyzed efficient production of single-stranded DNA nanostructures. *Chem.* **2021**, *7*, 959−981.
(13) Lu, J.; Hu, P.; Cao, L.; Wei, Z.; Xiao, F.; Chen, Z.; Li, Y.; Tian, L. Genetically Encoded and Biologically Produced All-DNA Nanomedicine Based on One-Pot Assembly of DNA Dendrimers for Targeted Gene Regulation. *Angew. Chem., Int. Ed.* **2021**, *60*, 5377−5385.
(14) Geary, C.; Rothemund, P. W.; Andersen, E. S. A single-stranded architecture for cotranscriptional folding of RNA nanostructures. *Science* **2014**, *345*, 799−804.
(15) Qi, X.; Zhang, F.; Su, Z.; Jiang, S.; Han, D.; Ding, B.; Liu, Y.; Chiu, W.; Yin, P.; Yan, H. Programming molecular topologies from single-stranded nucleic acids. *Nat. Commun.* **2018**, *9*, 4579.
(16) Li, M.; Zheng, M.; Wu, S.; Tian, C.; Liu, D.; Weizmann, Y.; Jiang, W.; Wang, G.; Mao, C. In vivo production of RNA nanostructures via programmed folding of single-stranded RNAs. *Nat. Commun.* **2018**, *9*, 2196.
(17) Ulyanov, N. B.; Ivanov, V. I.; Minyat, E. E.; Khomyakova, E. B.; Petrova, M. V.; Lesiak, K.; James, T. L. A pseudosquare knot structure of DNA in solution. *Biochemistry* **1998**, *37*, 12715−12726.
(18) Qian, H.; Yu, J.; Wang, P.; Dong, Q. F.; Mao, C. DNA cohesion through bubble−bubble recognition. *Chem. Commun.* **2012**, *48*, 12216−12218.

https://doi.org/10.1021/jacs.1c09925
J. Am. Chem. Soc. XXXX, XXX, XXX−XXX

Kinetic DNA Self-Assembly: Simultaneously Co-Folding Complementary DNA Strands into Identical Nanostructures

Mengxi Zheng, Zhe Li, Longfei Liu, Mo Li, Victoria E. Paluzzi, Jong Hyun Choi and Chengde Mao

Supporting Information

Experiment details

Oligonucleotides. All DNA strands were purchased from IDT, Inc. In all the template strands, the green, underlined sequences represent the primer-binding regions. The bold sequences represent the restriction enzyme cutting sites, while the red sequences represent a 90°-kink or bubble-bubble interaction regions. In the primer strands, the red sequences represent the regions that overlap with pUC19, the yellow sequences represent the regions that overlap with the 10-square-A fragment, and the blue sequences represent the regions of the 10-square-B fragments.

Name	Sequences
Forward primer	TTCTAATACGACTCACTATAGGTCTAGA
Reverse primer	TAGATTCTTAGCACTGCGAATTC
forward primer for 10-square-A	TGAATTCGAGCTCGGTACCC TCTAGATTGGGCAAGTACATCAAC
reverse primer for 10-square-A	AAAATTCTGT GGCGATACCTAGTTGAGCTAG
forward primer for 10-square-B	AGGTATCGCC ACAGAATTTTTAAGACAGGCGATAC
reverse primer for 10-square-B	GTCGACTCTAGAGGATCCCC CACTGCGAATTCCACTGACTC
Triangle-1	TTCTAATACGACTCACTATAGG**TCTAGA** TGACGGCATGATTGTTCGGAG AACTA CTCCTCTAGTCATCGAAG AGCCTATTTTTATCCGA CTTCGGTGACTGGAGGAG CTCTGAACAGTCATGTCGTCA GAGTGTGAG CTCGTCTAAGCATGACCTTGTCCAGGCTAG CTTGCC TAGGCTTTTTTTCGGAT GGCAAG AACTA CTAGCTTGGACGAGGTCGTGCTTGGACGAG AACTA CTCACACTC **GAATTC**GCAGTGCTAAGAATCTA

Triangle-2	TAGATTCTTAGCACTGC**GAATTC** GAGTGTGAG TAGTT CTCGTCCAAGCACGACCTCGTCCAAGCTAG TAGTT CTTGCC ATCCGAAAAAAAGCCTA GGCAAG CTAGCCTGGACAAGGTCATGCTTAGACGAG CTCACACTC TGACGACATGACTGTTCAGAG CTCCTCCAGTCACCGAAG TCGGATAAAAATAGGCT CTTCGATGACTAGAGGAG TAGTT CTCCGAACAATCATGCCGTCA **TCTAGA**CCTATAGTGAGTCGTATTAGAA
2-square-1	TTCTAATACGACTCACTATAGG**TCTAGA**CTTGCTTAGCA GGTGCAGCTGTAGGGTGTTC AACTA GGAAGGAAG AGCCTATTTTTATCCGA CTTCTTTCC GAACACTCTACAGTTGCACC T GGACTTGAGTCGAGCATGT T GCATCTTGTTGTAGCGATTC GGGC TAGGCTTTTTTTCGGAT GCCC AACTA GAATCGTTACAACGAGATGC CTTGGTTGGCTACTAGGTTC AACTA GGATCTGCC ACTCGATTTTTAGCTCA GGCGGATCC GAACCTGGTAGCCGACCAAG T ACATGTTCGACTTAAGTCC T TGCTGAGCAAG TGTTGGTCC GGCC TCGAGTTTTTTTGAGCT GGCC AACTA GGACTAACA **GAATTC**GCAGTGCTAAGAATCTA
2-square-2	TAGATTCTTAGCACTGC**GAATTC** TGTTAGTCC TAGTT GGCC AGCTCAAAAAAACTCGA GGCC GGACCAACA CTTGCTCAGCA A GGACTTAAGTCGAACATGT A CTTGGTCGGCTACCAGGTTC GGATCCGCC TGAGCTAAAAATCGAGT GGCAGATCC TAGTT GAACCTAGTAGCCAACCAAG GCATCTCGTTGTAACGATTC TAGTT GGGC ATCCGAAAAAAAGCCTA GCCC GAATCGCTACAACAAGATGC A ACATGCTCGACTCAAGTCC A GGTGCAACTGTAGAGTGTTC GGAAAGAAG TCGGATAAAAATAGGCT CTTCCTTCC TAGTT GAACACCCTACAGCTGCACC TGCTAAGCAAG **TCTAGA**CCTATAGTGAGTCGTATTAGAA
4-square-1	TTCTAATACGACTCACTATAGG**TCTAGA** AAGTAGAAGAGC GCAAGGTTCTGTCTTCACGT AACTA CGCATCGCC GTGTCATTTTTACTGTG GGCGATGCG ACGTGAGGACAGAGCCTTGC T GTGGATTCTCAAGCACTCC TT CGTACAGCGCTAGTAGATC T TCGCC TGACACTTTTTCACAGT GGCGA GCCATGCGG GCTAAGTTTTTGAATCG CCGCATGGC T GATCTATTAGCGTTGTACG TT CGATGGTGAGTGGTGATGC T CCTTAGGCCTATGTACCGCG ACGCC CTTAGCTTTTTCGATTC GGCGT AACTA CGCGGTGCATAGGCTTAAGG GCATCAGCTGTTTTACTGGT AACTA CGCATCGCC AGCCTATTTTTATCCGA GGCGATGCG ACCAGTGAAACAGTTGATGC T GCATCATCACTCATCATCG TT GCTTCTGTGGAACGAAGAC T TCGCC TAGGCTTTTTTTCGGAT GGCGA GCCATCGCC GACAGGTTTTTGGACAG GGCGATGGC T GTCTTTGTTCCATAGAAGC TT GGAGTGTTTGAGAGTCCAC T GCTCTTTTACTT TCCACTCG ACGCC CCTGTCTTTTTCTGTCC GGCGT AACTA CGAGTGGA **GAATTC**GCAGTGCTAAGAATCTA
4-square-2	TAGATTCTTAGCACTGC**GAATTC** TCCACTCG TAGTT ACGCC GGACAGAAAAAGACAGG GGCGT CGAGTGGA AAGTAAAAGAGC A GTGGACTCTCAAACACTCC AA GCTTCTATGGAACAAAGAC A GCCATCGCC CTGTCCAAAAACCTGTC GGCGATGGC TCGCC ATCCGAAAAAAAGCCTA GGCGA A GTCTTCGTTCCACAGAAGC AA CGATGATGAGTGATGATGC A GCATCAACTGTTTCACTGGT CGCATCGCC TCGGATAAAAATAGGCT GGCGATGCG TAGTT ACCAGTAAAACAGCTGATGC CCTTAAGCCTATGCACCGCG TAGTT ACGCC GAATCGAAAAAGCTAAG GGCGT CGCGGTACATAGGCCTAAGG A GCATCACCACTCACCATCG AA CGTACAACGCTAATAGATC A GCCATGCGG CGATTCAAAAACTTAGC CCGCATGGC TCGCC ACTGTGAAAAAGTGTCA GGCGA A GATCTACTAGCGCTGTACG AA GGAGTGCTTGAGAATCCAC A GCAAGGCTCTGTCCTCACGT CGCATCGCC CACAGTAAAAATGACAC GGCGATGCG TAGTT ACGTGAAGACAGAACCTTGC GCTCTTCTACTT **TCTAGA**CCTATAGTGAGTCGTATTAGAA

10-square-1	TTCTAATACGACTCACTATAGG**TCTAGA** TCGGGCAAGTACATC AACTA GGGATCGCC GCTAAGTTTTTGAATCG GGCGATCCC GATGTATTTGCCCGA CACTGATTCTCAGCC GAATGGTGTTGAATCCTGTGGTCGCAGCG TT GCTGGAAGCGGTTTATGTCCTGTGGAGTCC GAGACATGGATCGCC CTTAGCTTTTTCGATTC GGCGATTCATGTCTC AACTA GGACTCTACAGGATATAAACTGCTTCCAGC TT CGAACC CACTTTTTTTTTTTCAC GGTTCG TT GCTGTGTCGTGTTCAGAGC TT CGAGTCGTGCAGTGCTCCG TT GCTCAGGTGTAGGTGGTGC TT CGTCGCC AAAGTGTTTTTGTGAAA GGCGACG TT GCTGCAGATCAAGGTCCTC AACTA GGTACGG TTCGAATTTTTAAGCTT CCGTACC GAGGATCTTGATTTGCAGC TT CGCATAGGAGGAAGCTGGC TT CGACGTGTTGTCTTCATCC GAATGCC TTCGAATTTTTAAGCTT GGCATTC AACTA GGATGAGGACAACGCGTCG TT GCTGGTTTCGCATTGAATC AACTA GGTAGCC GACAGGTTTTTGGACAG GGCTACC GATTCGATGCGAGACCAGC TT CGTACC GTGTCATTTTTACTGTG GGTACG TT GCCAGTTTCCTCTTATGCG TT GCACCATCTACACTTGAGC TT CGAGGGTCTACTGCGTTCG TT GCTAGCC TGACACTTTTTCACAGT GGCTAGC TT CGTCACGCGTCTCGGATCC GATAGCC CCTGTCTTTTTCTGTCC GGCTATC AACTA GGATCTGAGACGTGTGACG TT GCATTTGAGAGTGCTTGGC TT CGATCAGCTGCAATGCTTCCTATCTCTTC AACTA GGACTGGGAAGCGGAGGAAGTGACTAGCTC AACTA GGTATCGCC ACAGAATTTTTAAGACA GGCGATACC GAGCTAGTCGCTTCCTTCGCTTCTCAGTCC GAAGAGATGGGAAGCGTTGCAGTTGATCG TT GCCTGACGTTCGAATCGCTTTGAGTGAGCC GAGTGGTTAGTCGCC TTCTGTTTTTTTGTCTT GGCGATTAACCACTC AACTA GGCTCATTCAAAGTGATTCGGACGTCAGGC TT CGTGCC AGAAGATTTTTAGAAGA GGCACG TT GCCAAGTACTCTCGAATGC TT CGAACGTAGTAGATCCTCG TT GCTGACTCTGAGGGAAGGC TT CGTTGCC TCTTCTTTTTTTCTTCT GGCAACG TT GCTGTATATGAGAGCTCTC AACTA GGTTGCC CCATTATTTTTATTACC GGCAACC GAGAGTTCTCATGTACAGC TT CGACCTGCGTCCAGTTGCG TT GCCATCTTCAACCGTTCCC GAACGCC TAATGGTTTTTGGTAAT GGCGTTC AACTA GGGAATGGTTGAGGATGGC TT CGAACTCTGTCTGTCCCTC AACTA GGTAGCC TAGGCTTTTTTTCGGAT GGCTACC GAGGGATAGACAGGGTTCG TT GCTGCC ACTCGATTTTTAGCTCA GGCAGC TT CGCAATTGGACGTAGGTCG TT GCCTTTCCTCAGGGTCAGC TT CGGAGTACTGCATGACTCG TT GCAAGCC TCGAGTTTTTTTGAGCT GGCTTGC TT CGTGAAGGTGACTGAGACC GAAGCGG AGCCTATTTTTATCCGA CCGCTTC AACTA GGTCTTAGTCACTTTCACG TT GCTCTGGACACGATACAGC TT CGCTGCGATCACAGGGTTCAACGCCATTC AACTA GGCTGAGAGTCAGTG **GAATTC**GCAGTGCTAAGAATCTA
10-square-2	TAGATTCTTAGCACTGC**GAATTC** CACTGACTCTCAGCC TAGTT GAATGGCGTTGAACCCTGTGATCGCAGCG AA GCTGTATCGTGTCCAGAGC AA CGTGAAAGTGACTAAGACC TAGTT GAAGCGG TCGGATAAAAATAGGCT CCGCTTC GGTCTCAGTCACCTTCACG AA GCAAGCC AGCTCAAAAAAACTCGA GGCTTGC AA CGAGTCATGCAGTACTCCG AA GCTGACCCTGAGGAAAGGC AA CGACCTACGTCCAATTGCG AA GCTGCC TGAGCTAAAAATCGAGT GGCAGC AA CGAACCCTGTCTATCCCTC GGTAGCC ATCCGAAAAAAAGCCTA GGCTACC TAGTT GAGGGACAGACAGAGTTCG AA GCCATCCTCAACCATTCCC TAGTT GAACGCC ATTACCAAAAACCATTA GGCGTTC GGGAACGGTTGAAGATGGC AA CGCAACTGGACGCAGGTCG AA GCTGTACATGAGAACTCTC GGTTGCC GGTAATAAAAATAATGG GGCAACC TAGTT GAGAGCTCTCATATACAGC AA CGTTGCC AGAAGAAAAAAAGAAGA GGCAACG AA GCCTTCCCTCAGAGTCAGC AA CGAGGATCTACTACGTTCG AA GCATTCGAGAGTACTTGGC AA CGTGCC TCTTCTAAAAATCTTCT GGCACG AA GCCTGACGTCCGAATCACTTTGAATGAGCC TAGTT GAGTGGTTAATCGCC AAGACAAAAAAACAGAA GGCGACTAACCACTC GGCTCACTCAAAGCGATTCGAACGTCAGGC AA CGATCAACTGCAACGCTTCCCATCTCTTC GGACTGAGAAGCGAAGGAAGCGACTAGCTC GGTATCGCC

	TGTCTTAAAAATTCTGT GGCGATACC TAGTT GAGCTAGTCACTTCCTCCGCTTCCCAGTCC TAGTT GAAGAGATAGGAAGCATTGCAGCTGATCG AA GCCAAGCACTCTCAAATGC AA CGTCACACGTCTCAGATCC TAGTT GATAGCC GGACAGAAAAAGACAGG GGCTATC GGATCCGAGACGCGTGACG AA GCTAGCC ACTGTGAAAAAGTGTCA GGCTAGC AA CGAACGCAGTAGACCCTCG AA GCTCAAGTGTAGATGGTGC AA CGCATAAGAGGAAACTGGC AA CGTACC CACAGTAAAAATGACAC GGTACG AA GCTGGTCTCGCATCGAATC GGTAGCC CTGTCCAAAAACCTGTC GGCTACC TAGTT GATTCAATGCGAAACCAGC AA CGACGCGTTGTCCTCATCC TAGTT GAATGCC AAGCTTAAAAATTCGAA GGCATTC GGATGAAGACAACACGTCG AA GCCAGCTTCCTCCTATGCG AA GCTGCAAATCAAGATCCTC GGTACGG AAGCTTAAAAATTCGAA CCGTACC TAGTT GAGGACCTTGATCTGCAGC AA CGTCGCC TTTCACAAAAACACTTT GGCGACG AA GCACCACCTACACCTGAGC AA CGGAGCACTGCACGACTCG AA GCTCTGAACACGACACAGC AA CGAACC GTGAAAAAAAAAAAGTG GGTTCG AA GCTGGAAGCAGTTTATATCCTGTAGAGTCC TAGTT GAGACATGAATCGCC GAATCGAAAAAGCTAAG GGCGATCCATGTCTC GGACTCCACAGGACATAAACCGCTTCCAGC AA CGCTGCGACCACAGGATTCAACACCATTC GGCTGAGAATCAGTG TCGGGCAAATACATC GGGATCGCC CGATTCAAAAACTTAGC GGCGATCCC TAGTT GATGTACTTGCCCGA **TCTAGA**CCTATAGTGAGTCGTATTAGAA

DNA Sequence Design. When designing the DNA sequences, the critical part of each structure included the bubble-bubble interaction, the 90°-kink loop, the 3-way junctions, and the 4-way junctions. These were first designed with specific sequences to ensure the formation of the defined nanostructures. The remaining duplex regions were assigned with random sequences by software Tiamat[1]. For duplex regions longer than 11 basepairs, every 5-6 bases, one of the Watson-Crick basepairs (A-T or G-C) was replaced by a G-T wobble base pair to weaken the secondary structures and facilitate PCR amplification of the DNA templates. Primers binding regions, including one XbaI and one EcoRI restriction enzyme sites, were added at the 5′- and 3′- ends to allow PCR amplification and plasmid cloning. To further confirm the design, the folding of ssDNAs were predicted by the Mfold server.[2] For designs that amplified via plasmid cloning, the restriction enzyme cutting site maps were checked to ensure the unique cleavage site of the enzymes XbaI and EcoRI.

Polymerase chain reaction. The DNA double-stranded template was amplified by a polymerase chain reaction using Taq DNA polymerase kit (New England Biolabs Inc.). 4 ng DNA template, 200 μM dNTPs, 0.2 μM of forward and reverse primers, and 0.5 μL (2.5 units) Taq DNA polymerase were mixed in 100 μL of standard Taq reaction buffer (10 mM Tris-HCl, 50 mM KCl, 1.5 mM $MgCl_2$, pH 8.3). The reaction mixture was transferred to the PCR cycler preheated to 95 °C and underwent the thermocycle: initial denaturation, a 95 °C, 30 Cycles of 95 ℃ for 30s, 54 °C for 30s and 68 °C for 1-2 min. The final extension is set to be 68 °C for 5 min.

Purification of dsDNA. 5% denaturing PAGE gel was prepared with the 19:1 acrylamide/bisacrylamide solution, 8 M urea, and TBE buffer, containing 89 mM Tris base (pH 8.0), 89 mM boric acid, and 2 mM EDTA. The gel was run at 55 °C with a voltage of 650 V on Hoefer SE 600 electrophoresis system and was stained with ethidium bromide (Sigma). The major band was cut under UV light and eluted out.

Formation of ssDNA nanostructures for native PAGE analysis. 0.5 μg of dsDNAs

(30 nM triangle, or 20 nM 2-square, or 12.5 nM 4-square, or 4.5 nM 10-square dsDNAs) were prepared in 100 μL TAE buffer (40 mM Tris base, 20 mM acetic acid, 2 mM EDTA). The 100 μL solution was divided into 5 tubes equally, heated to 95 °C for 5 min and rapidly transferred to an ice bath for another 5 min. The 5 tubes of 20 μL solutions were then mixed together, followed by the addition of 25 μL TAE/50 mM Mg^{2+} buffer (40 mM Tris base, 20 mM acetic acid, 2 mM EDTA, and 52.5 mM magnesium acetate) to reach the final Mg^{2+} concentration of 10 mM. For the triangles, 300 nM of the forward primer and 300 nM of the reverse primer were pre-mixed with 30 nM of the dsDNA while 200 nM primers were added when preparing 2-square nanostructures.

Native PAGE. 4% native PAGE gel was prepared with 19:1 acrylamide/bisacrylamide gel and TAE/Mg^{2+} buffer (40 mM Tris base, 20 mM acetic acid, 2 mM EDTA, and 12.5 mM magnesium acetate) or TBE buffer. The gel was run at 4 °C. Then stained with Stains-All (Sigma) and scanned by an HP scanner (Scanjet 4070 Photosmart).

Formation of ssDNA nanostructures for AFM imaging. 5nM of dsDNAs were prepared in 20 μL TAE buffer (40 mM Tris base, 20 mM acetic acid, 2 mM EDTA). The solutions were first heated to 95 °C for 5 min and rapidly transferred to an ice bath for another 5 min, followed by the addition of 20 μL TAE/20 mM Mg^{2+} buffer (40 mM Tris base, 20 mM acetic acid, 2 mM EDTA, and 22.5 mM magnesium acetate) to reach the final Mg^{2+} concentration of 10 mM. To ensure the quality the AFM images, the primers were not added when preparing the triangle and 2-square samples for the AFM imaging. The samples were visualized right after the preparation to avoid the hybridization of the complementary nanostructures into long dsDNAs.

AFM imaging. The mica surface (Ted Pella, Inc.) was pre-treated with 10 mM Ni^{2+} to increase the adsorption of ssDNA nanostructures. 20 μL of 10 mM $NiCl_2$ was added onto the freshly cleaved mica substrate and was incubated for 5 min, followed by 20 μL of pure water to wash the surface. 5 μL of the DNA solution was deposited on the dried mica surface and incubated for 2 mins. 20 μL TAE/Mg^{2+} buffer was further added. AFM images were captured by MultiMode 8 (Bruker) using ScanAsyst-fluid mode with ScanAsyst-fluid+ probes (Bruker). For the PCR mixture samples, after depositing the sample onto the mica surface and incubating for 2 mins, the solution mixture was dried by compressed air and washed with 20 μL TAE/Mg^{2+} buffer three times.

4-square Recombinant plasmid preparation. The dsDNA and pUC19 plasmid (GenScript Inc.) were double digested by XbaI and EcoRI restriction enzymes (New England BioLabs Inc.), respectively. The DNA was recovered by DNA clean & concentrator columns (Zymo Research Corp.) to remove the salt and enzymes. Then the dsDNA insert and plasmid vector were ligated by T4 DNA ligase (New England BioLabs Inc.), and were incubated overnight at 25 °C.

10-square Recombinant plasmid preparation. The two 10-square fragments (10-square-A and 10-square-B) were obtained by PCR amplification using the 10-square dsDNA template and two pairs of primers (10-square-A forward primer and 10-square-A reverse primer; 10-square-B forward primer and 10-square-B reverse primer). 0.2 pmoles of 10-square-A and 10-square B were then mixed with the SmaI linearized pUC19 vector in a 1:1:1 ratio. Then, the prepared 20 μL mixture of the three DNA fragments in 1 × HiFi DNA Assembly Master Mix (New England Biolabs Inc.) was incubated at 50°C for

60 minutes for subsequent transformation.

Plasmid cloning and bacteria amplification. The ligation product was combined with MAX Efficiency™ DH5α Competent *E. coli* for transformation (Thermo Fisher Scientific). The mixture was incubated on ice for 30 min, and then heated to 42 °C for 90 s and put on ice for 2 min. 900 μL of room temperature S.O.C. medium was added into the solution and shaken at 37 °C for 1 hour at the speed of 220 rpm. The transformed bacteria were spread on LB Broth (Thermo Fisher Scientific, LB Broth, Powder (Lennox)) plates containing 100 μg/ml ampicillin and incubated overnight at 37 °C. After the colonies grew into the desired size, colonies were randomly chosen, and transferred into individual aliquots of 6 ml LB/ampicillin liquid medium and shook overnight at 37 °C. The plasmid was extracted using Zyppy Plasmid Miniprep Kits (Zymo Research Corp.). The extracted plasmid was characterized by restriction enzyme digestion and the correct insert was purified using the PAGE (for 4-square DNA) and the agarose gel electrophoresis (for 10-square DNA).

Agarose gel analysis. 1% agarose gel with TAE/Mg^{2+} buffer or TBE buffer is used to analysis and the purified 10-square fragments. The gel electrophoresis was performed on a FB-SB-710 electrophoresis unit (FisherBiotech) at 4 °C under a constant voltage of 80 V. The gel was stained in EB and illuminated under UV light.

Reference

1. Sean Williams, Kyle Lund, Chenxiang Lin, Peter Wonka, Stuart Lindsay, and Hao Yan. Tiamat: a three-dimensional editing tool for complex DNA structures. In International workshop on DNA-based computers, 90-101. Springer, Berlin, Heidelberg, **2008**.
2. Michael Zuker. "Mfold web server for nucleic acid folding and hybridization prediction." *Nucleic Acids Res*. **31**, 3406-3415 (2003).

	Sequence	Complementary Sequence
1	AGCCTA	TAGGCT
2	ACTCGA	TCGAGT
3	CGTACA	TGTACG
4	GAGATC	GATCTC
5	ATCATG	CATGAT
6	GTGTCA	TGACAC
7	ACAGAA	TTCTGT
8	CCATTA	TAATGG
9	CACTTT	AAAGTG
10	TTCGAA	TTCGAA
11	GACAGG	CCTGTC
12	AGAAGA	TCTTCT
13	GCTAAG	CTTAGC

Table S1. The sequences of the 13 pairs of bubble-bubble interactions. To minimize the cross interaction between each pair of bubbles, the continuous mismatches between each bubble were designed to be no more than three and the total mismatches were less than 6 basepairs.

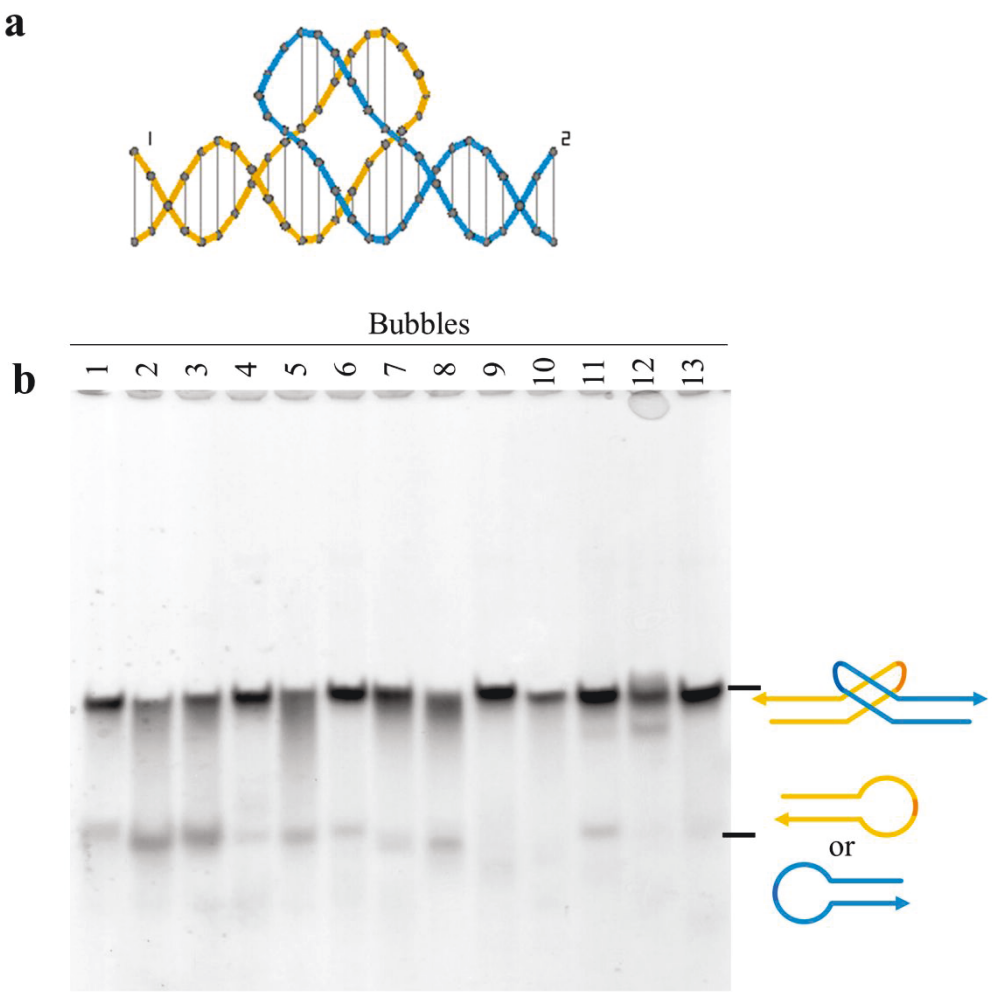

Figure S1. Bubble-bubble interactions. **a)** A scheme of the bubble-bubble interactions. **b)** Native PAGE analysis of the thirteen pairs of bubbles listed in Table S1. In some pairs of bubbles, the left-over monomer bands reveal the low binding efficiencies. However, this will not have an impact on the construction of self-folding structures, as they are used as intra-molecular joints. The relative low binding affinities are negligible when the two bubbles are adjacent to each other, confined by the overall shape of the self-folded structures.

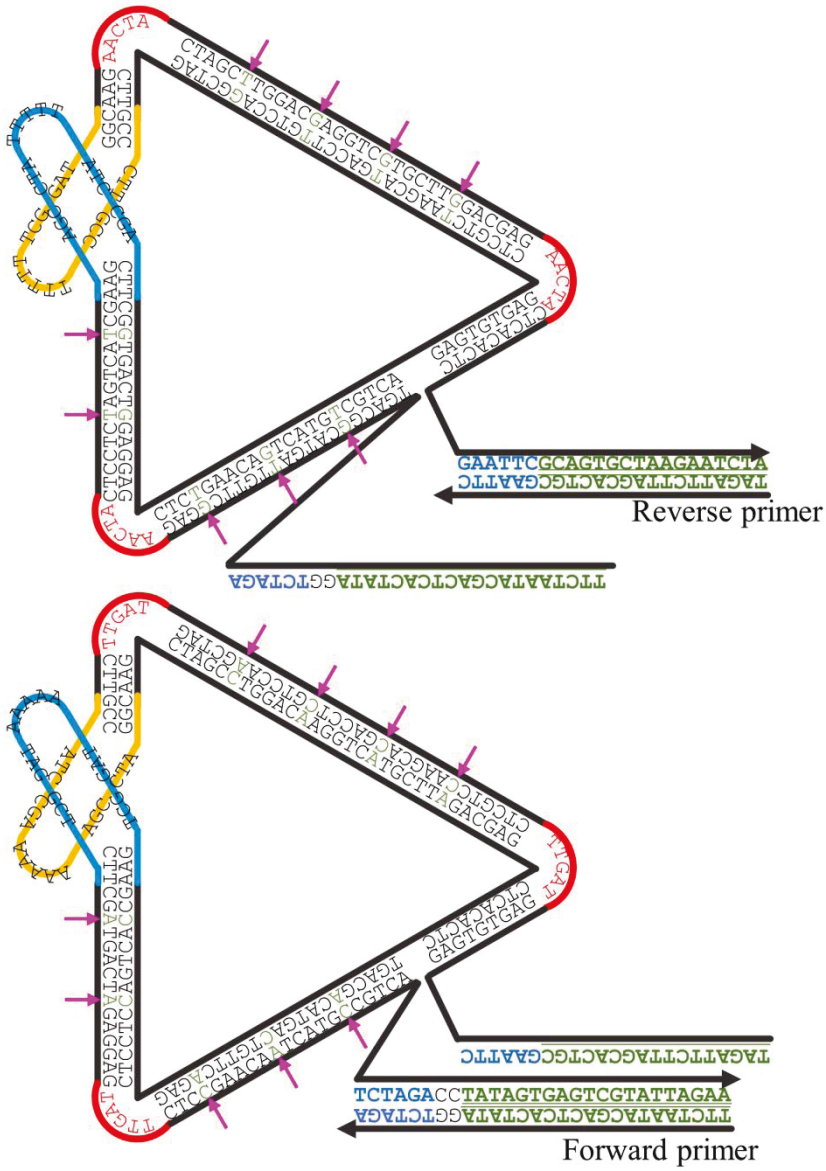

Figure S2. The secondary DNA structures of a pair of triangles. Underlined bases are the primer binding sites for PCR reactions. The G-T mismatches and A-C mismatches are indicated using magenta arrows.

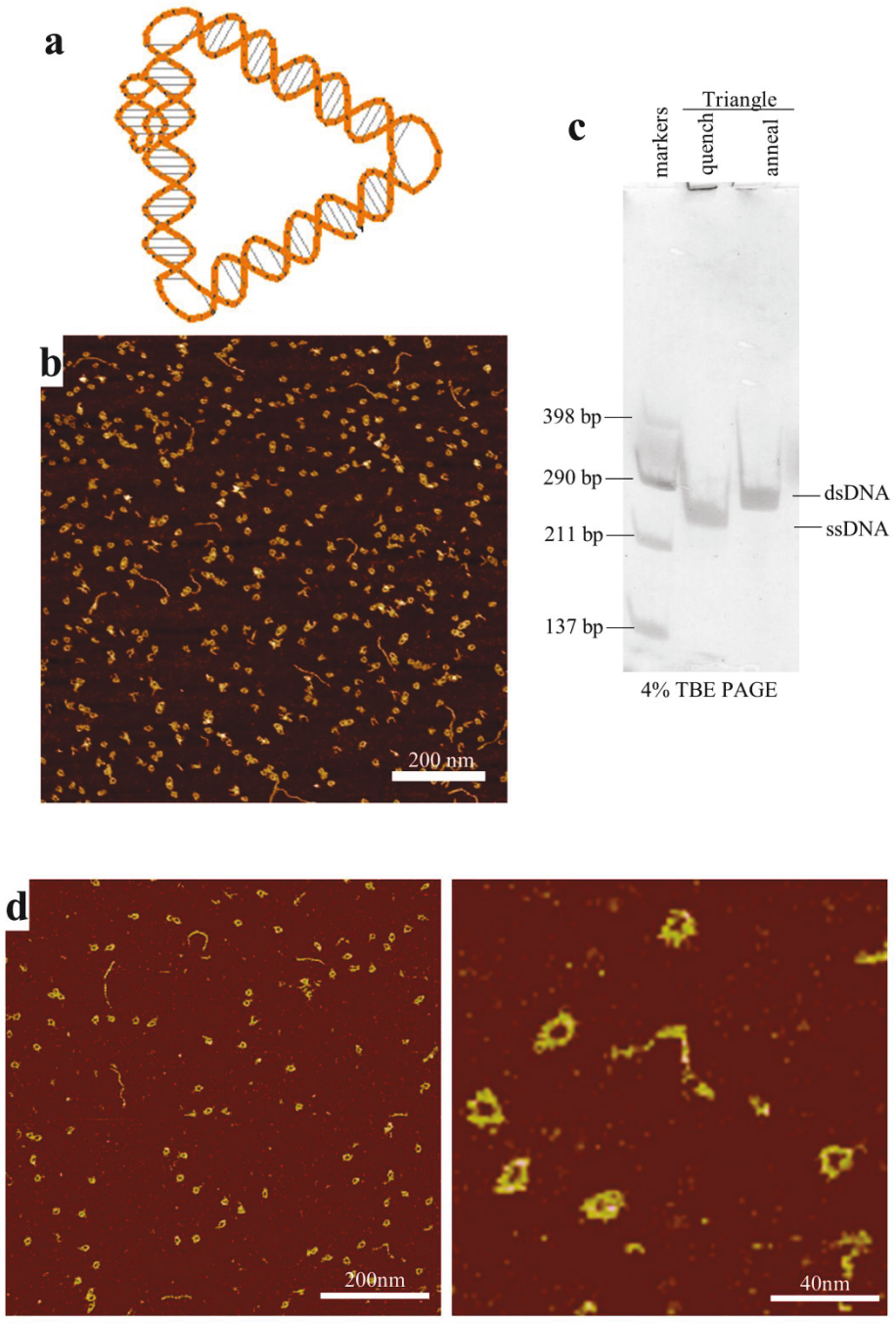

Figure S3. The DNA triangles were prepared from purified dsDNA. (a) A structural scheme of the main body. (b) A large-field view of the AFM image (in the presence of Mg^{2+}), (c) native PAGE analysis of the heat-quench products of dsDNA in the absence of Mg^{2+} and PCR primers. (d) A pair of AFM images at two different magnifications of DNA triangles resulting from a PCR mixture.

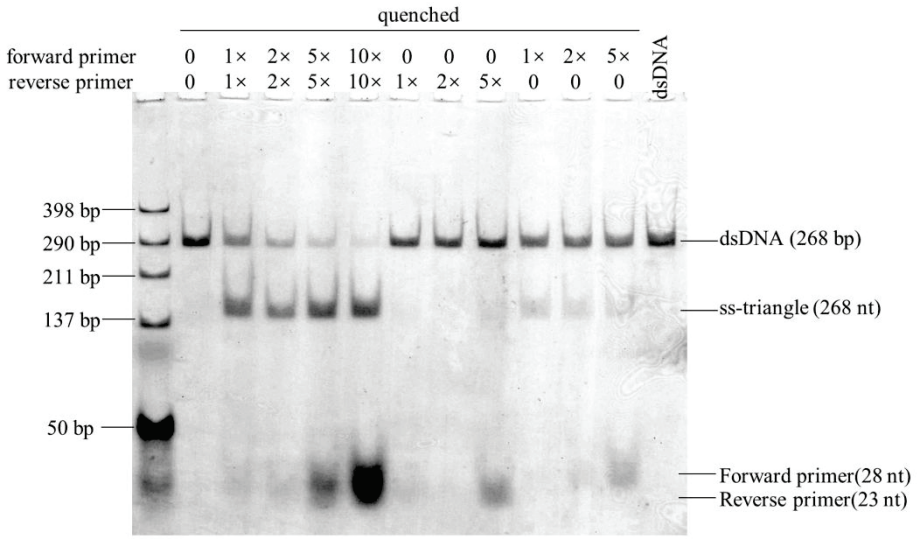

Figure S4. The effect of primers on the DNA triangles. N× means N-fold of the primers in relation to the dsDNA concentration were added into the sample while preparing the solution. The dsDNA concentrations were 30 nM. All the samples were incubated at 25 °C for 24 hours before the PAGE analysis.

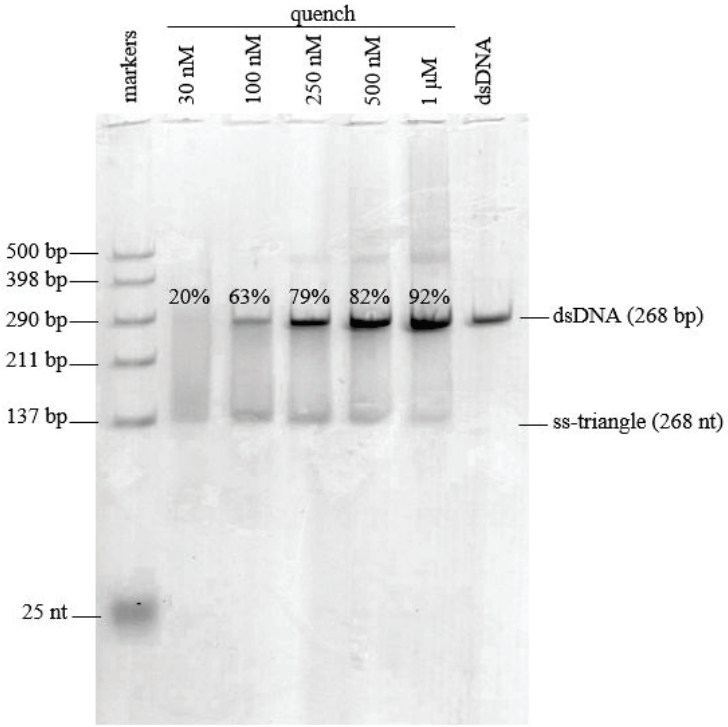

Figure S5. The formation of the DNA triangles with different DNA concentrations. The samples do not contain any primers to protect the tails at the 5' and 3' ends. The percentages of the dsDNA existed in the sample were semi-quantitatively estimated from the band intensities.

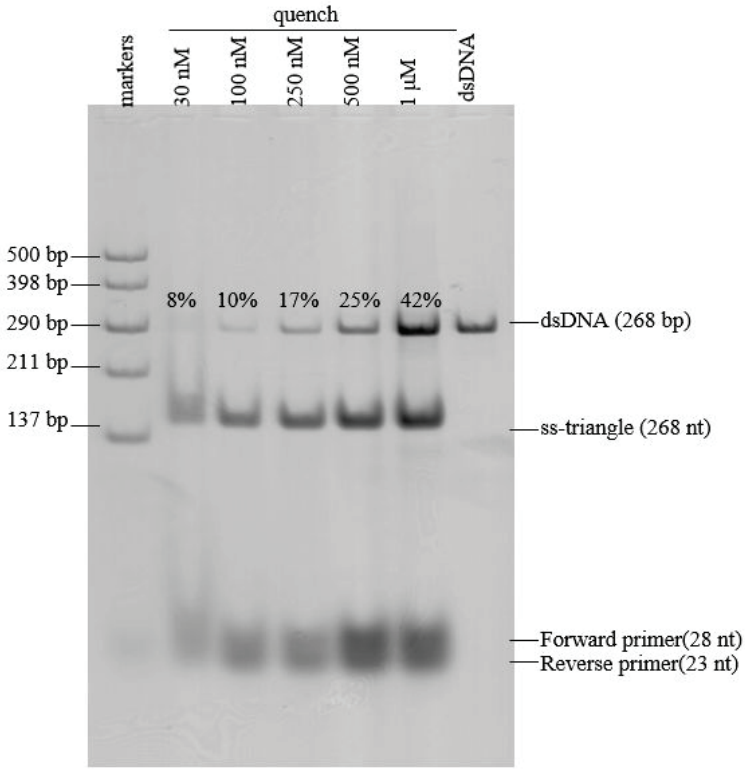

Figure S6. The formation of the DNA triangles with different DNA concentrations. The samples contain 10-fold of the forward and reverse primers to protect the tails at the 5' and 3' ends, except the 1 μM sample. The 1μM sample contains 5 μM of primers (5-fold) instead of 10 μM (10-fold).

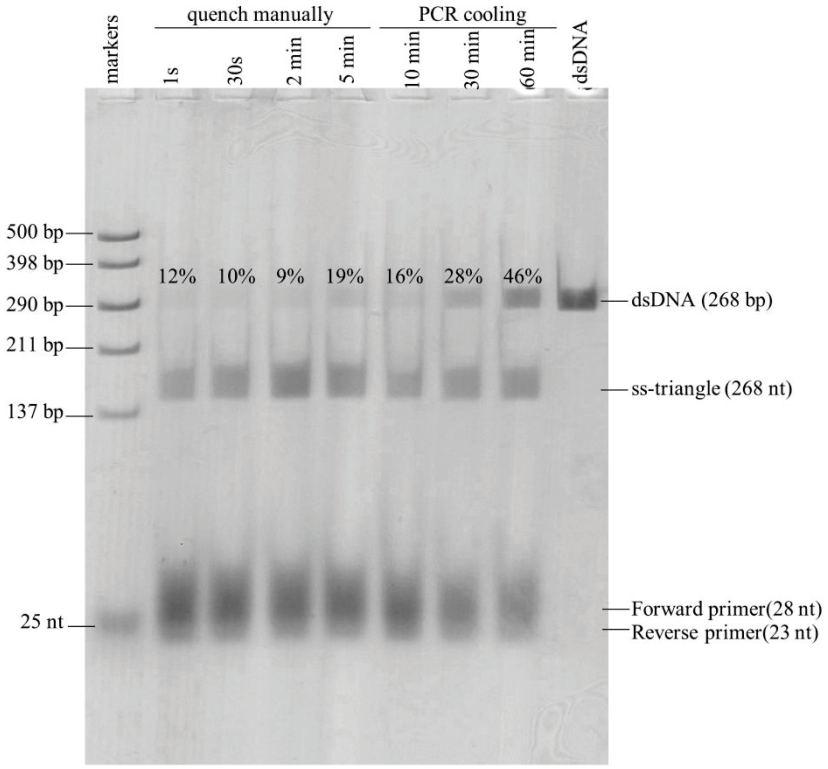

Figure S7. Native polyacrylamide gel electrophoresis analysis of the formation of the DNA triangles with different cooling ramps. The samples contain 10-fold of the forward and reverse primers to bind with the tails at the 5' and 3' ends.

Quench manually: The samples were manually moved from 95 °C to 65 °C to 50 °C to 37 °C heating blocks, then to a 25 °C room temperature tube holder, and finally a 0 °C ice bath.

Lane **1s**, 95°C /5 min → ice bath.

Lane **30s**: 95°C /5 min → 65°C /5s, 50°C /5s, 37°C /5s, 25°C /5s→ ice bath.

Lane **2 min**: 95°C /5 min → 65°C /30s, 50°C /30s, 37°C /30s, 25°C /30s→ ice bath.

Lane **5 min**: 95°C /5 min → 65°C /75s, 50°C /75s, 37°C /75s, 25°C /75s→ ice bath

PCR cooling: The fastest cooling rate that our PCR cycler allows is ~10 min.

Lane **10 min**: 95°C /5 min → 1°C.

Lane **30 min**: 95°C /5 min → 80°C /2.5min, 70°C / 2.5min, 60°C / 2.5min, 50°C / 2.5min, 40°C / 2.5min, 30°C / 2.5min, 20°C / 2.5min, 10°C / 2.5min → 1°C

Lane **60 min**: 95°C /5 min → 80°C /6min, 70°C / 6min, 60°C / 6min, 50°C / 6min, 40°C / 6min, 30°C / 6min, 20°C / 6min, 10℃/ 6min → 1°C

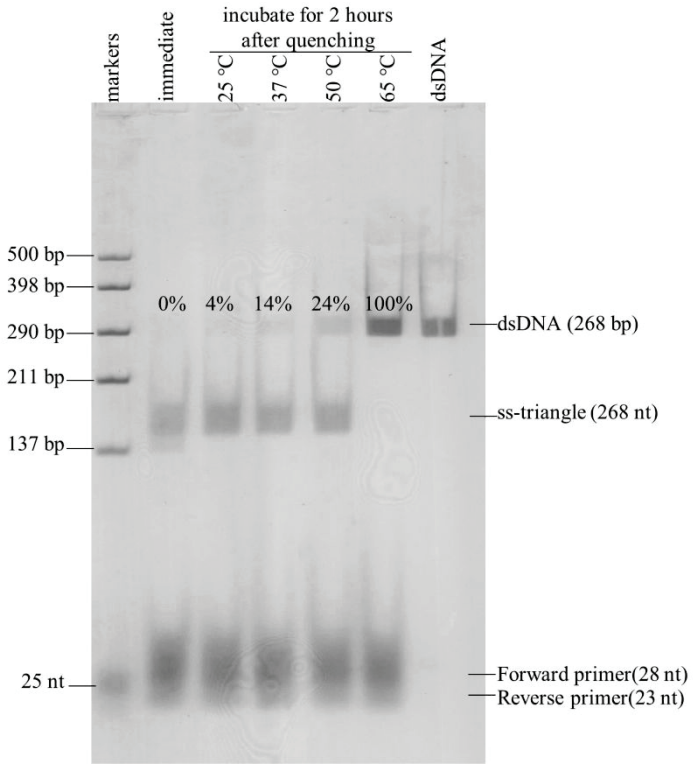

Figure S8. The thermal stability of DNA triangles at different temperatures. After quenching, the DNA triangles were incubated at 25, 37, 50, and 65 °C for 2 hours.

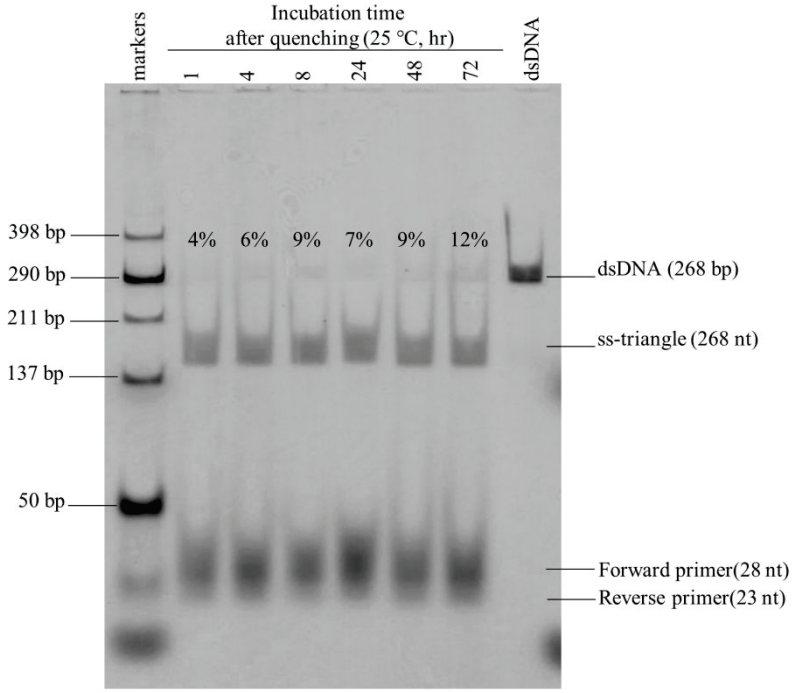

Figure S9. The stability of the folded DNA triangles at 25 °C over 72 hours. After quenching, the samples are incubated at 25 °C for designated times before PAGE analysis.

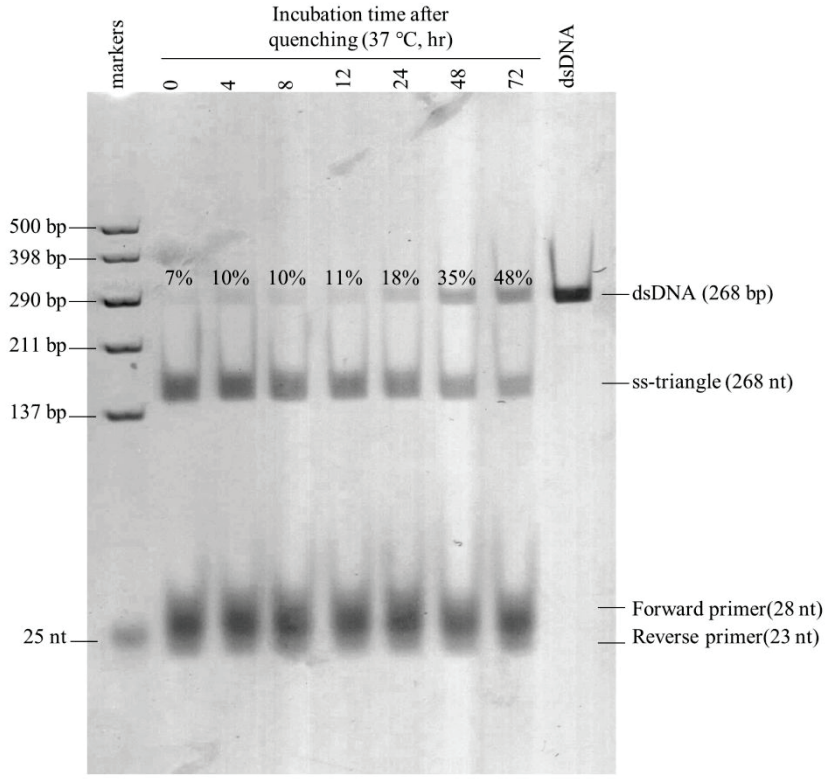

Figure S10. The stability of the folded DNA triangles at 37 °C over 72 hours. After quenching, the samples are incubated at 37 °C for designated times before PAGE analysis.

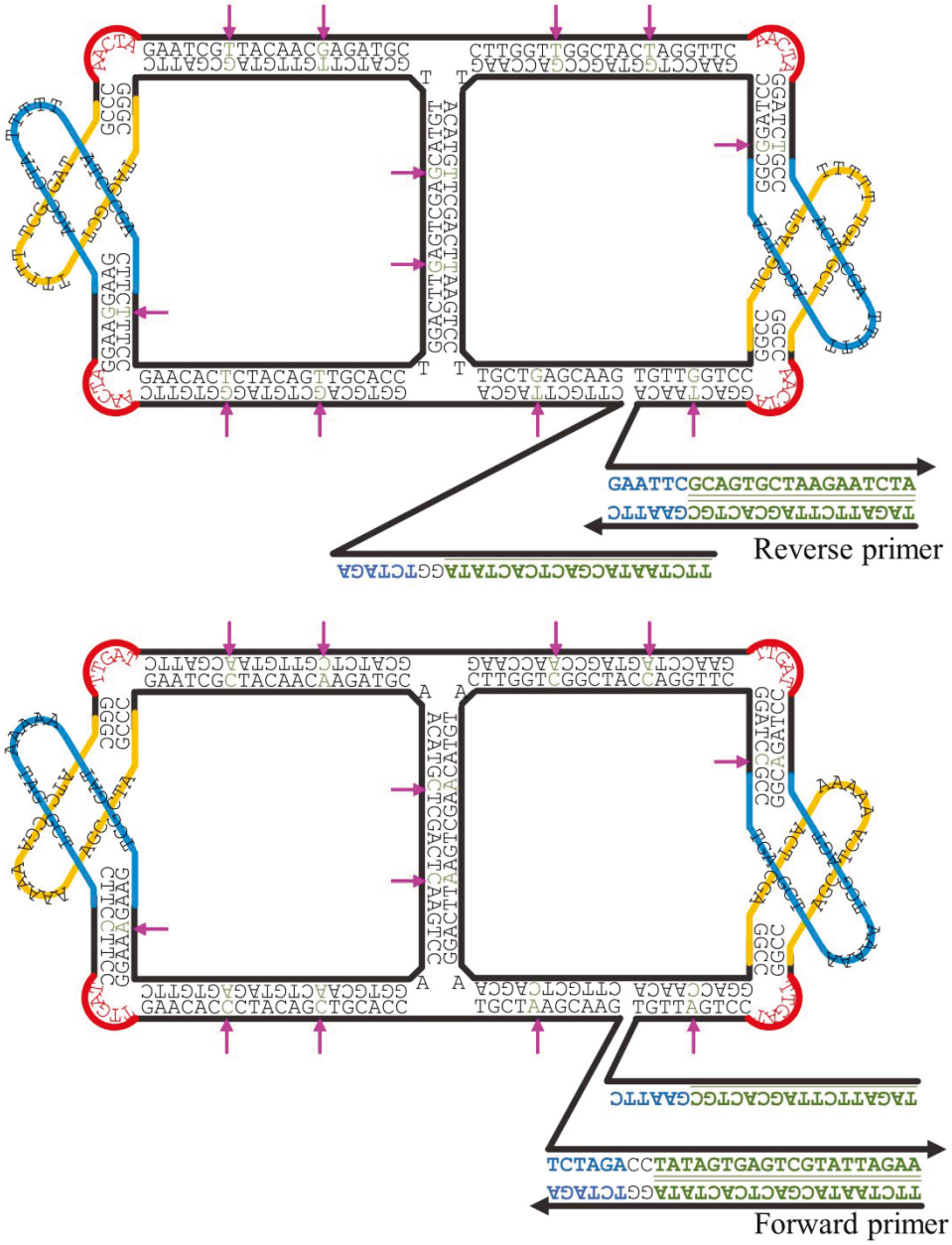

Figure S11. The secondary DNA structures of a pair of 2-squares. Underlined bases are the primer binding sites for PCR reactions. The G-T mismatches and A-C mismatches are indicated using magenta arrows.

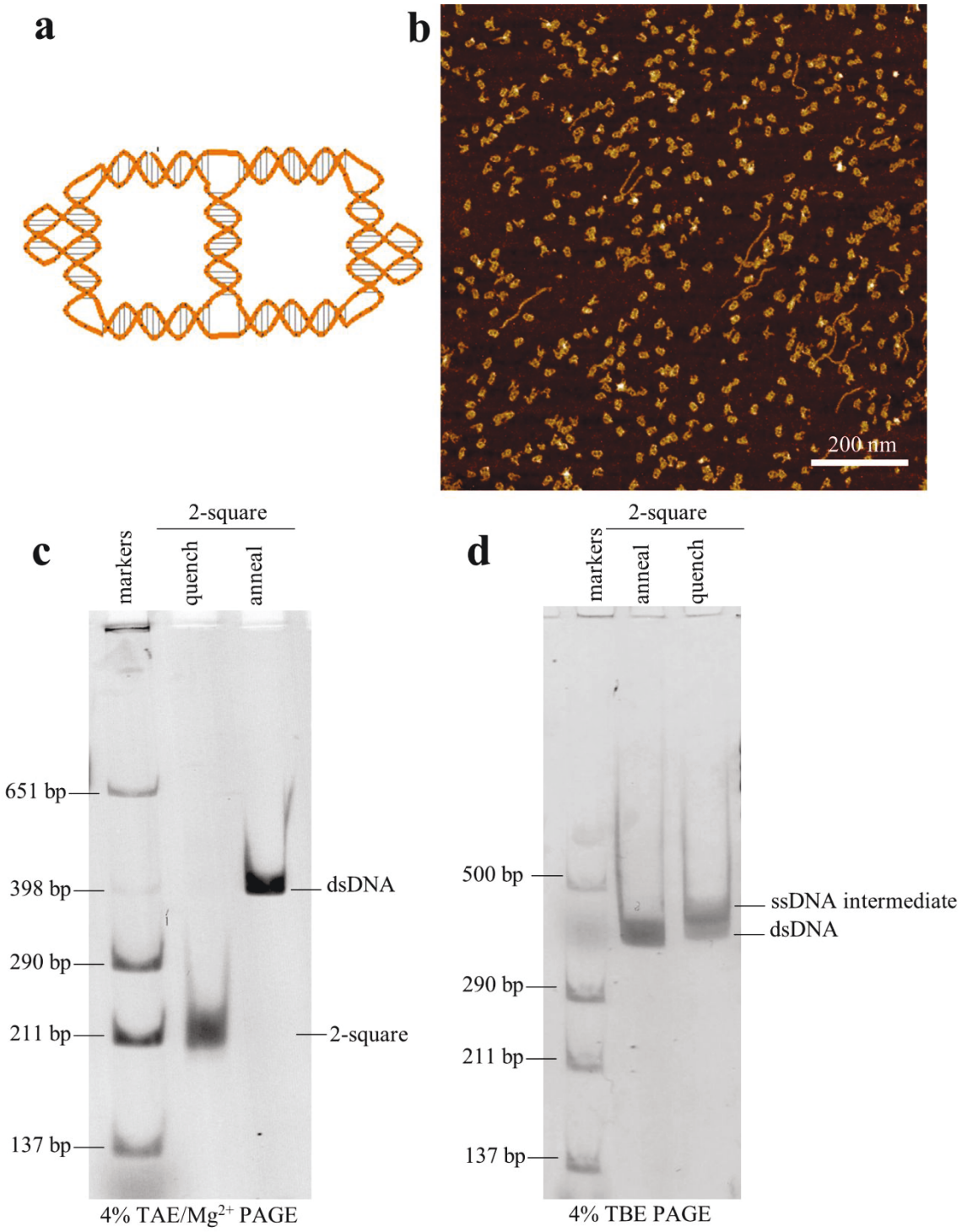

Figure S12. The DNA 2-sqaures prepared from purified dsDNA. (a) A structural scheme of the main body. (b) A large-field view of the AFM image (in the presence of Mg^{2+}), native PAGE analysis of the heat-quench products of dsDNA with PCR primers (c) in the presence of 10 mM Mg^{2+} and (d) in the absence of Mg^{2+}. In (c) the folding yield is estimated to be 95.6% by Image J.

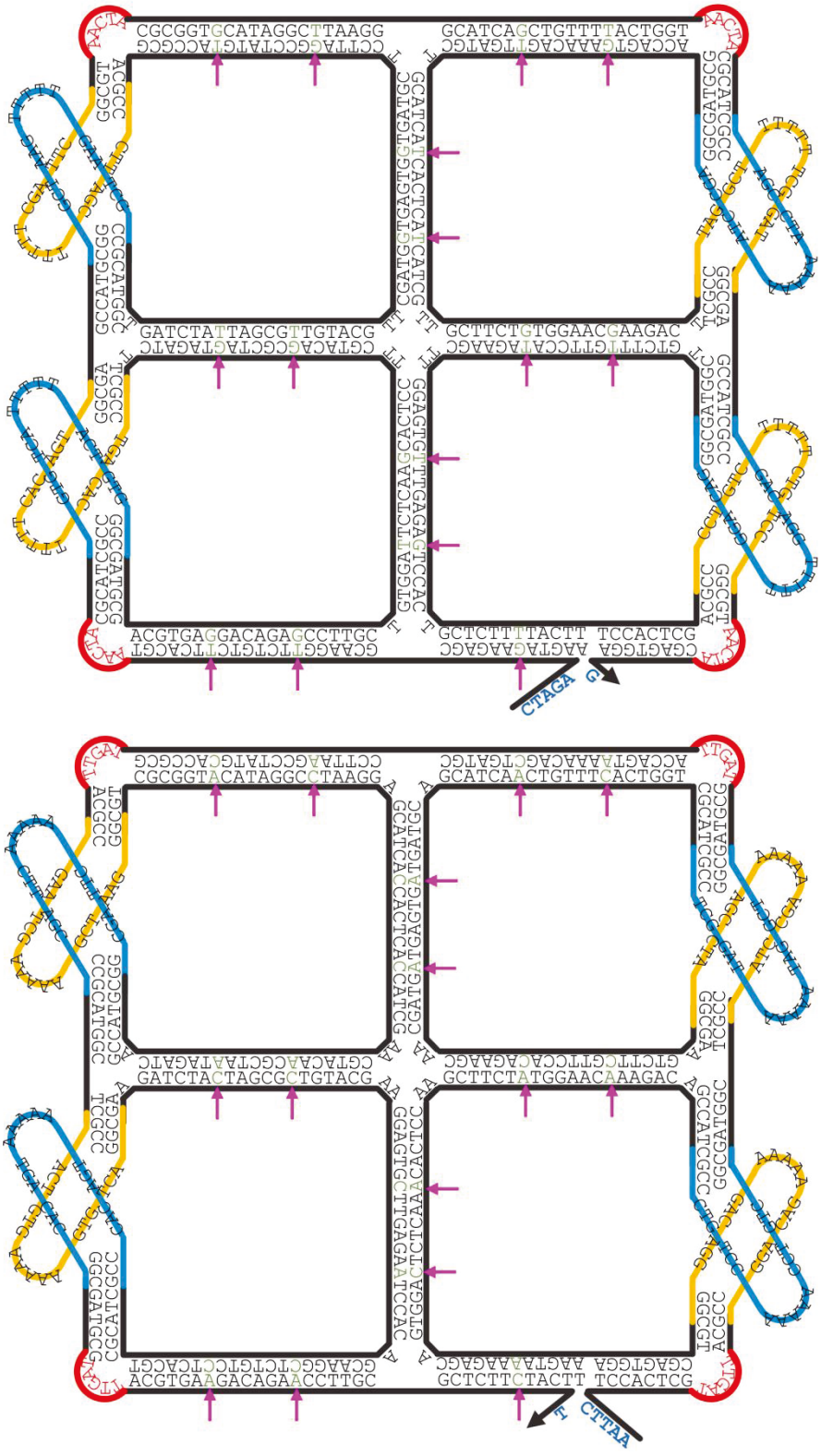

Figure S13. The secondary DNA structures of a pair of 4-squares. Underlined bases are the primer binding sites for PCR reactions. The G-T mismatches and A-C mismatches are indicated using magenta arrows.

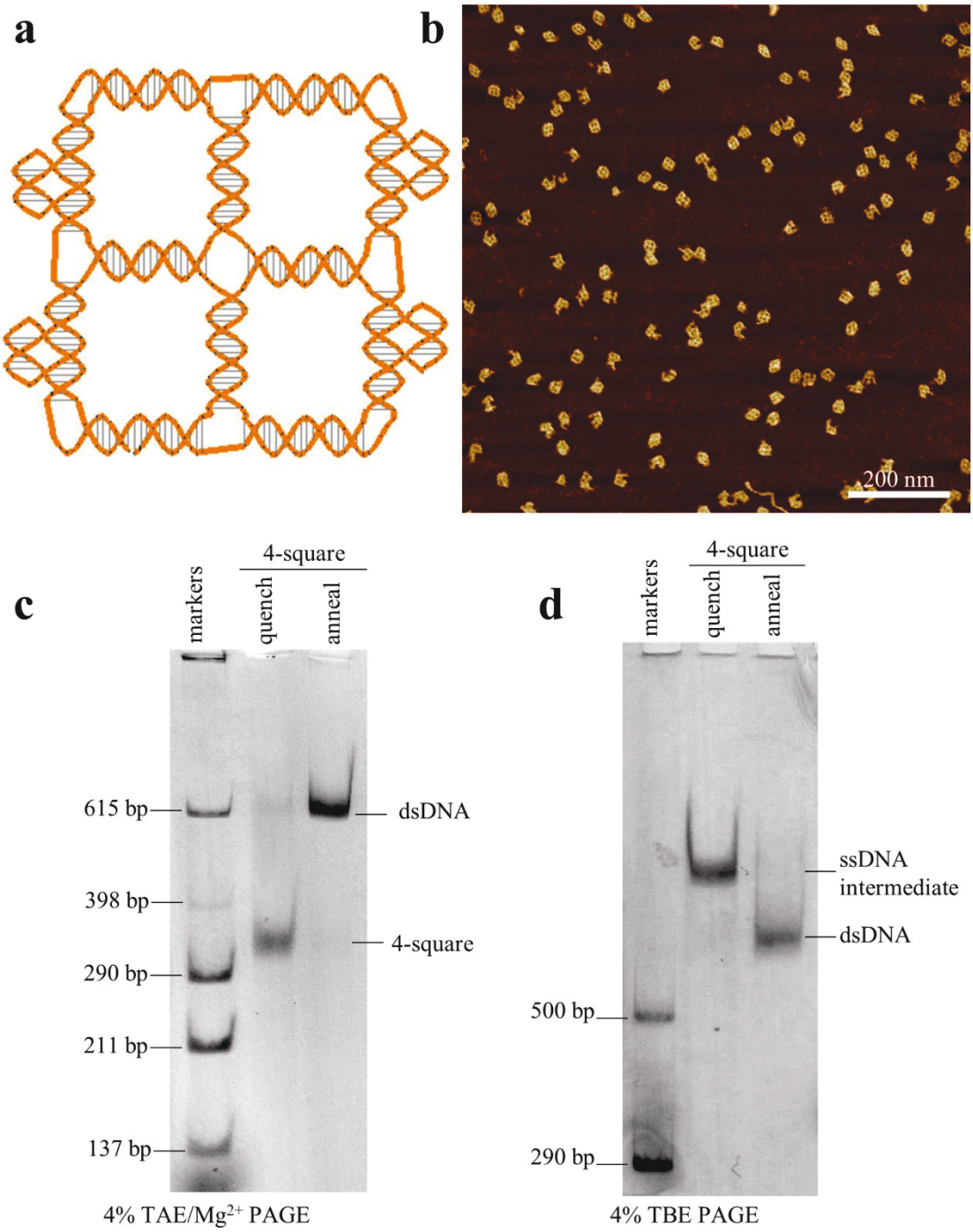

Figure S14. The DNA 4-sqaures prepared from purified dsDNA. (a) A structural scheme of the main body. (b) A large-field view of the AFM image (in the presence of Mg^{2+}), native PAGE analysis of the heat-quench products of dsDNA (c) in the presence of 10 mM Mg^{2+} and (d) in the absence of Mg^{2+}. In (c) the folding yield is estimated to be 93.3% by Image J.

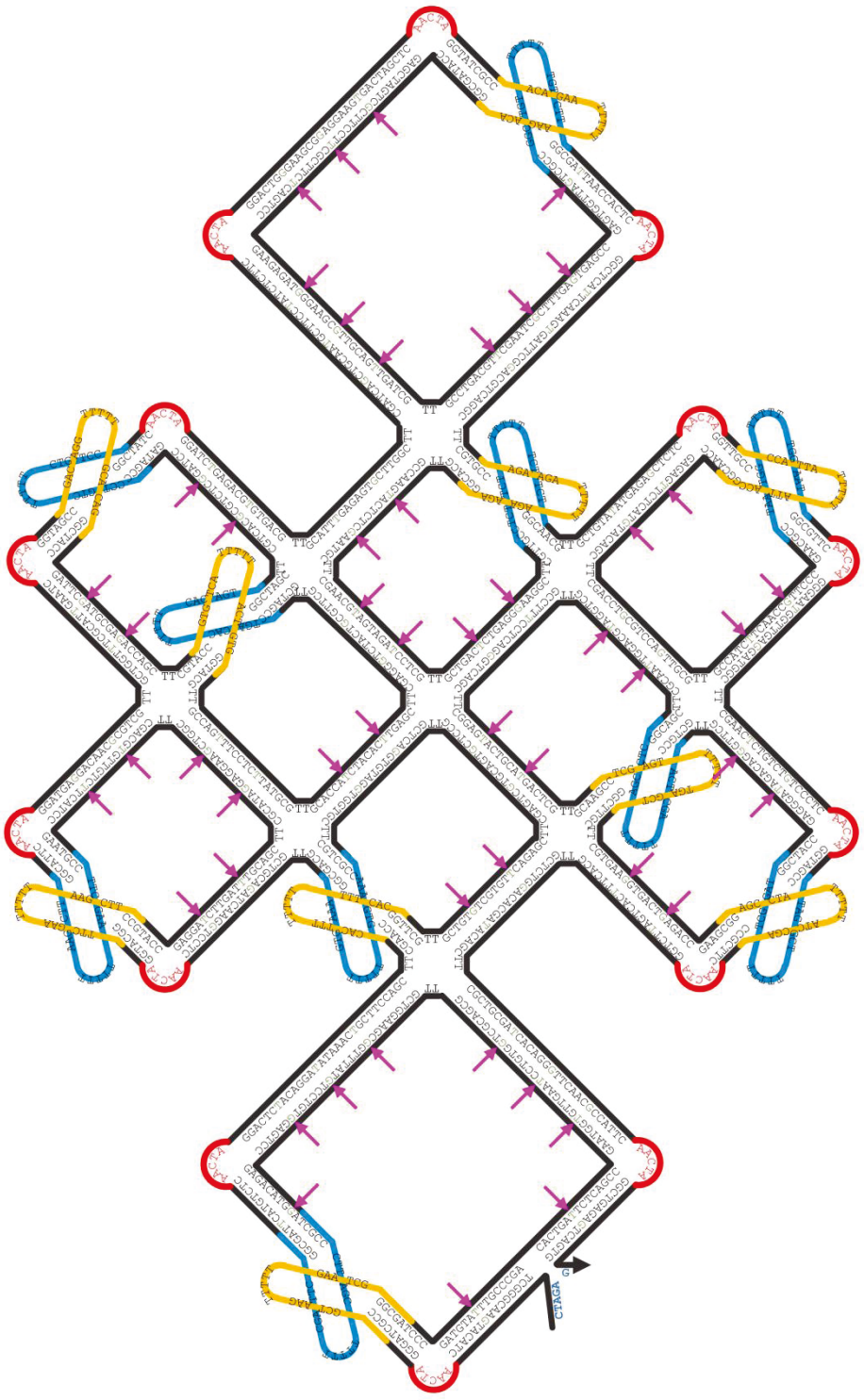

Figure S15-1. The secondary DNA structure of 10-square. The G-T mismatches and A-C mismatches are indicated using magenta arrows.

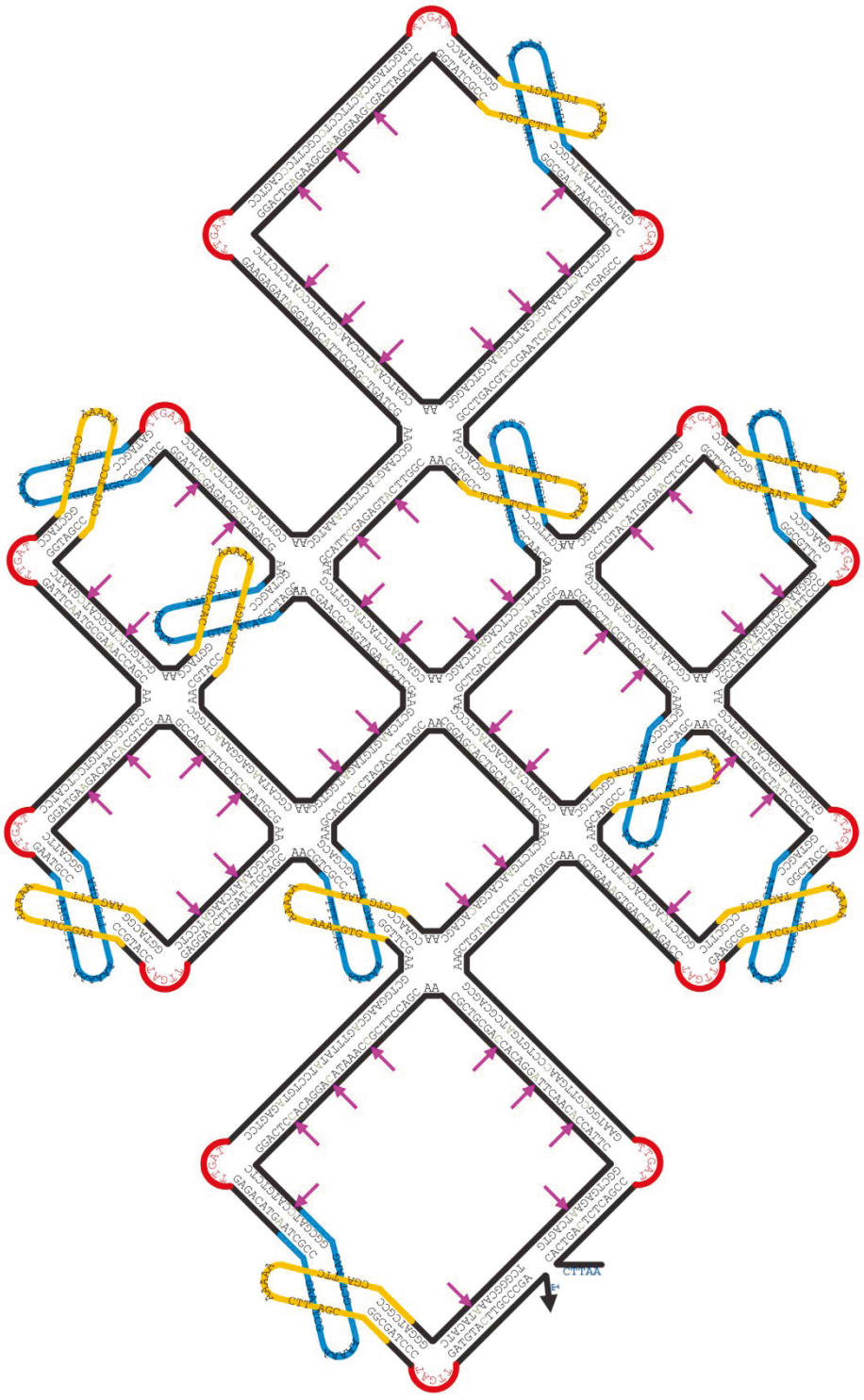

Figure S15-2. The secondary DNA structure of 10-square. The G-T mismatches and A-C mismatches are indicated using magenta arrows.

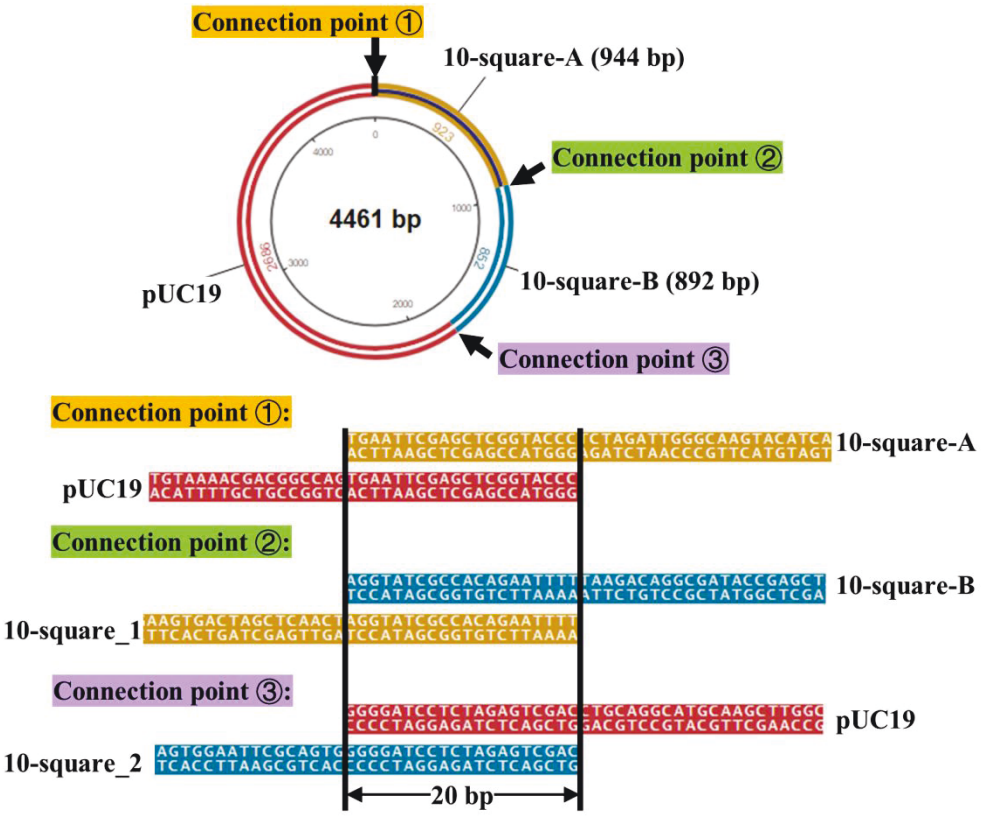

Figure S16. The construction of the recombinant 10-square-pUC19 plasmid using NEB HiFi assembly. To amplify the 10-square structures, the NEB HiFi assembly cloning method was used instead of the traditional cloning method. The failure of applying the traditional cloning method on the 10-square DNA was speculated to be the strong secondary structures of the dsDNA. To assemble pUC19 (red) and two fragments (yellow and blue) into a circular plasmid, three DNAs were designed to have 20-bp overhangs that were the same sequence with each other at the connection point 1,2 and 3, respectively. The pUC19 plasmid was linearized by SmaI restriction enzymes, while the 10-square dsDNA template was amplified into two fragments using PCR with two pairs of designed primers. The fragment **10-square-A** (yellow) is 944-bp and fragment **10-square-B** is 892-bp.

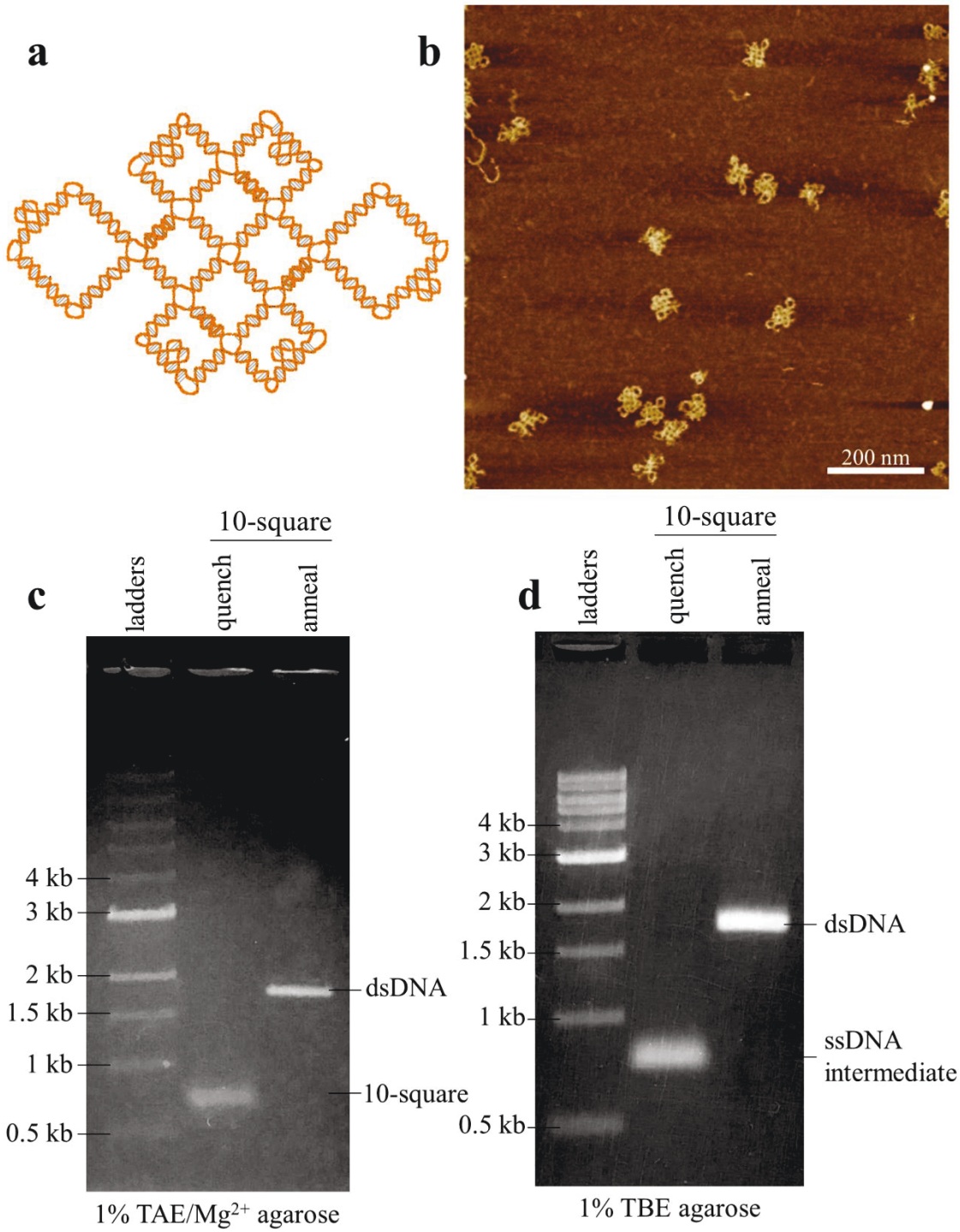

Figure S17. The DNA 10-sqaures prepared from purified dsDNA. (a) A structural scheme of the main body. (b) A large-field view of the AFM image (in the presence of Mg^{2+}), native PAGE analysis of the heat-quench products of dsDNA (c) in the presence of 10 mM Mg^{2+} and (d) in the absence of Mg^{2+}. In (c) the folding yield is estimated to be 100% by Image J.

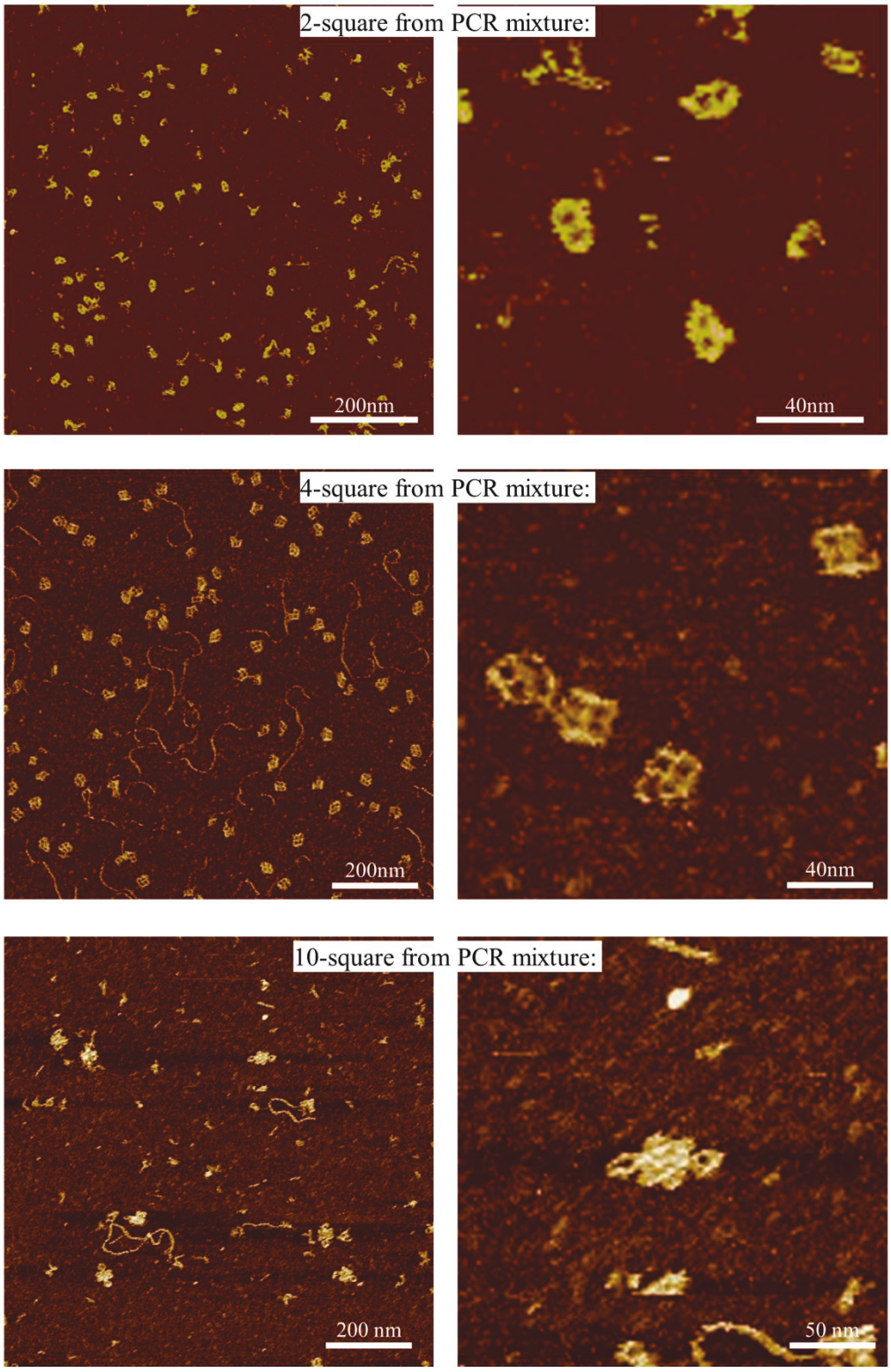

Figure S18. The AFM images of complex DNA structures resulting from the PCR mixtures. For each structure, a pair of AFM images at two different magnifications are shown.

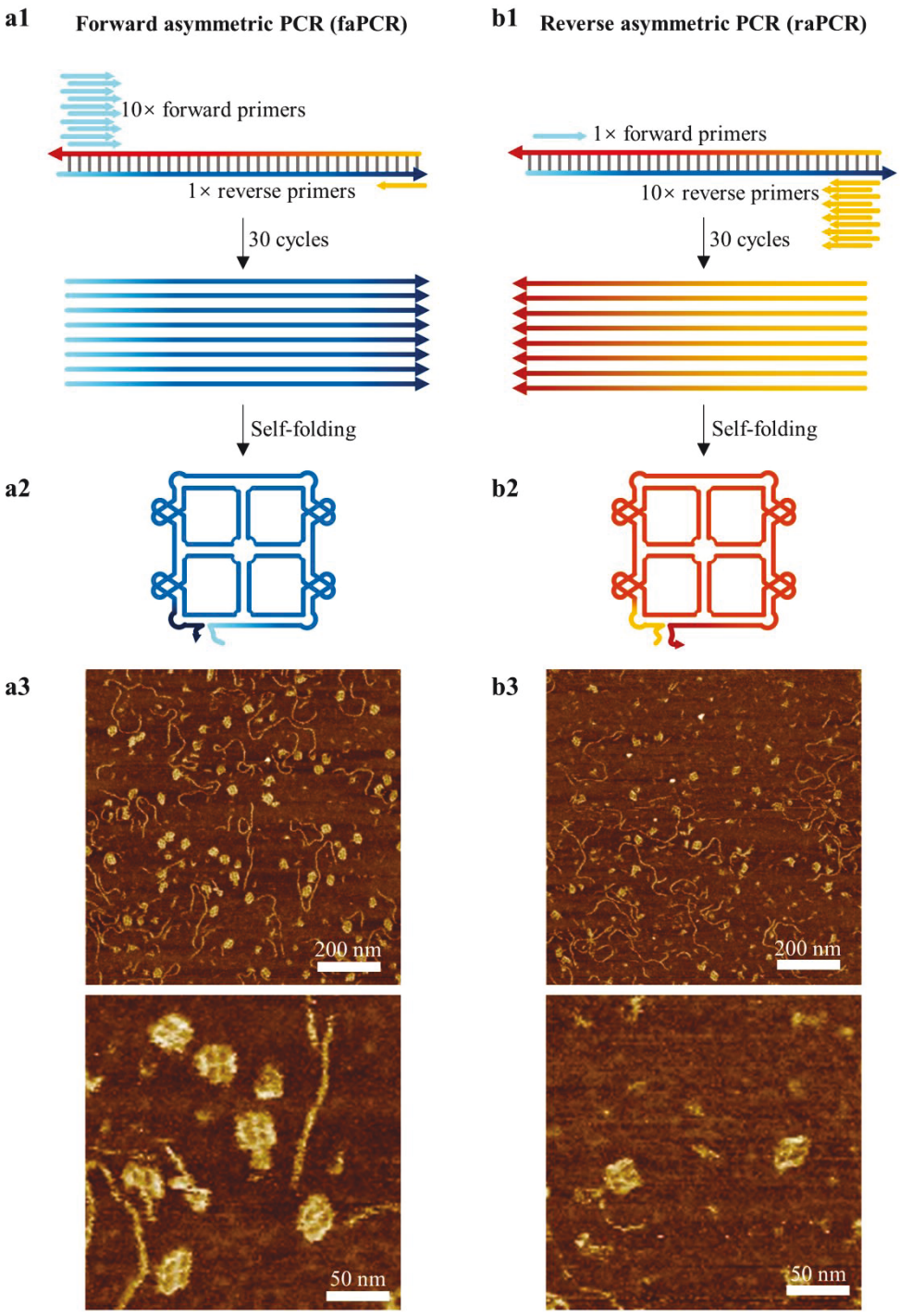

Figure S19. Separately folding of the DNA 4-squares from ssDNAs prepared by asymmetric PCR (aPCR) reactions. (a) From the top strand and (b) from the bottom strand. (a1) & (b1) Forward aPCR (faPCR) and reverse aPCR (raPCR), respectively. (a2) & (b2) Folded 4-square structures from faPCR and raPCR, respectively. (a3) & (b3) A pair of AFM images at different magnifications of the faPCR mixture and raPCR mixture.

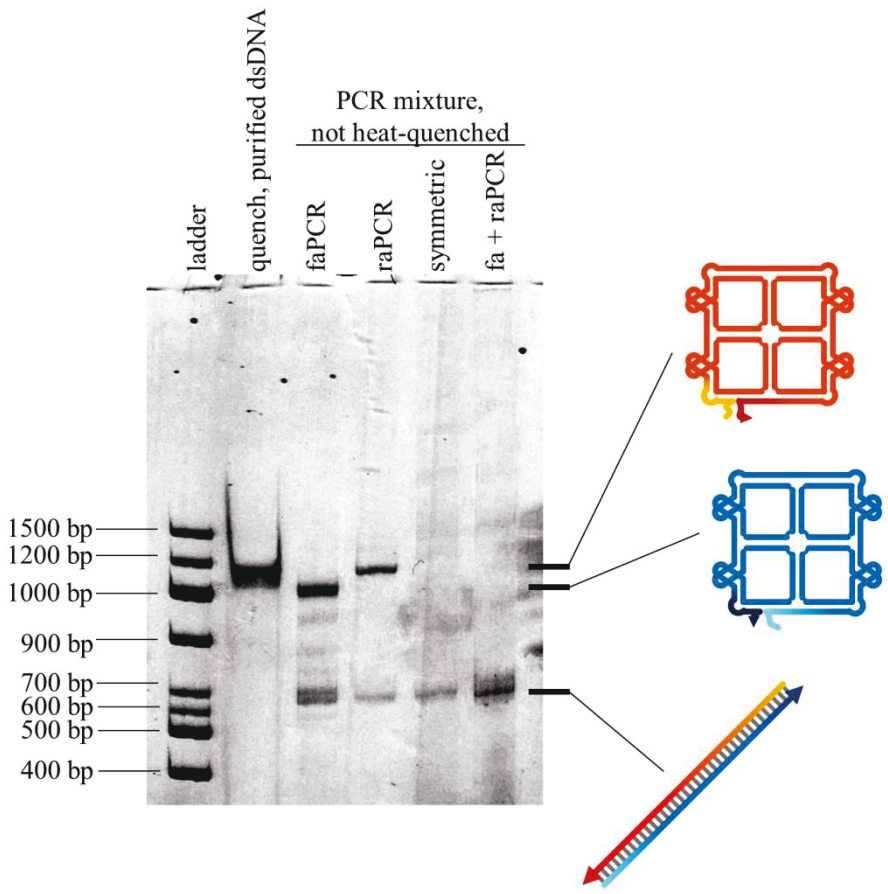

Figure S20. The TBE polyacrylamide gel electrophoresis of the asymmetric PCR product of 4-square dsDNA. Lane 1: ladder; Lane 2: purified 4-square dsDNA was quenched; Lane 3: asymmetric PCR mixture of 4-square dsDNA (Forward primer: reverse primer = 10:1); Lane 4: asymmetric PCR mixture of 4-square dsDNA (Forward primer : reverse primer = 1:10); Lane 5: symmetric PCR mixture of 4-square dsDNA; Lane 6: the mixture of Lane 3 and 4. In all DNA solutions, there was an excess amount of PCR primers.